Subsidence dynamics of the Montney Formation (Early Triassic, Western Canada Sedimentary Basin): insights for its geodynamic setting and wider implications

Sébastien Rohais, Vincent Crombez, Tristan Euzen, John-Paul Zonneveld

Subsidence dynamics of the Montney Formation (Early Triassic, Western Canada Sedimentary Basin): insights for its geodynamic setting and wider implications

Sébastien ROHAIS

IFP Energies nouvelles, 1 et 4 Avenue de Bois-Préau, 92852 Rueil-Malmaison Cedex, France

Vincent CROMBEZ

IFP Energies nouvelles, 1 et 4 Avenue de Bois-Préau, 92852 Rueil-Malmaison Cedex, France

Tristan EUZEN

IFP Technologies (Canada) Inc., Suite 810, 744 - 4th Avenue S.W., Calgary, AB T2P 3T4, Canada

John-Paul ZONNEVELD

Ichnology Research Group, Department of Earth and Atmospheric Sciences, 1-26 Earth Sciences Building, University of Alberta, Edmonton, Alberta, Canada T6G2E3

ABSTRACT

This study presents the first published subsidence analysis during the deposition of the Montney Formation. It was deposited during the Early Triassic (ca. 252.2-245 Ma) in the Western Canadian Sedimentary Basin (WCSB) located along the western margin of the North American craton. Subsidence analyses of six representative wells and two outcrop sections along a proximal to distal transect are presented using a backstripping method integrating recent high-resolution stratigraphic correlations for the Montney Formation. The entire Paleozoic to

Cenozoic sedimentary column of the WCSB was backstripped to put the deposition of the Montney Formation into a broader context and provide results regarding the type of subsidence and geodynamic setting for the Montney Formation.

The spatial and temporal evolution of the subsidence during the deposition of the Montney Formation indicates that the most likely basin setting is a foreland. The tectonic subsidence during the Triassic is herein interpreted as a combination of the topographic loading of the orogenic wedge (flexure) and the sublithospheric ''loading'' caused by slab load-driven subsidence (dynamic subsidence). This suggests that the retro-foreland basin setting was associated with an eastward dipping subduction during the deposition of the Montney Fm.

Three foreland stages are thus recorded in the whole WCSB, with evidence for (1) a Late Permian (fore-arc) pro-foreland setting, then (2) a Triassic collisional retro-foreland basin prior to the well-known (3) Jurassic-Cenozoic collisional retro-foreland.

INTRODUCTION

The Canadian Cordillera is very well known for their terranes and the associated collisional retro-foreland traditionally interpreted to be initiated during the Mid-Jurassic. Two main stages are classically inferred to describe their tectonic evolution (Price, 1994 and reference herein) with a first (1) Late Proterozoic to Jurassic "miogeocline-platform" stage where the Western Canada Sedimentary Basin (WCSB) is described as a "passive margin", and a subsequent (2) Jurassic to Eocene collisional foreland stage. Transition from one stage to the other should be easily recognized especially because passive margin and foreland are two

extreme end-members of basin evolution. This transition may involve complex scenarios. Multiple interpretations have been proposed and debated for the Permian to Triassic periods in Canada during which the Montney Formation (Early Triassic) was deposited. For instance, the paleogeographic maps published by Miall and Blakey (2008) suggest a back-arc setting that is also supported by other studies (e.g. Zonneveld et al., 2010). Controversy, the new series of paleogeographic maps published by Blakey (2014) suggest a pro-foreland in a fore-arc setting based on the work of Nelson et al. (2006), Colpron et al. (2007) and Mortensen et al. (2007). Recently, Onoue et al. (2015) suggest that the Upper Triassic was deposited in a distal ramp environment on the passive western margin of the North American craton. The debate about the geodyamic setting is mainly related to three key issues for the entire North American Cordillera orogen: 1) what was the exact location of the different terranes including island arcs, oceanic crust and small cratonic masses during the Paleozoic (e.g. Monger and Price, 1979; Coney et al., 1980, Monger et al., 1982; Johnston and Borel, 2007; Beranek and Mortensen, 2011; Colpron et al., 2015) ? 2) What was the type and timing of initial accretion and was the margin cylindrical, i.e. could we export the Antler-Sonoma orogeny evolution from North America to the Canadian Cordillera (e.g. Speed and Sleep, 1982; Oldow et al., 1989; Barclay, 2000; Mortensen et al., 2007; Fuentes et al., 2009; Sigloch and Mihalynuk, 2013) ? 3) What was the timing and amplitude of post-Triassic large oblique-slip displacement (e.g. Gabrielse, 1985; Irving et al., 1985; Engebretson et al., 1985; Saleeby and Busby-Spera, 1992; Dickinson, 2004) ?

While most of these scenarios are based on geological mapping, volcanic and magmatic occurrences, structural restoration and geodynamic reconstruction of exotic terranes, little evidence has been derived from the sedimentary record in

the WCSB to document and constrain the timing of deformation. Beranek and Mortensen (2007, 2011) and Colpron et al. (2015) published geological mapping and sediment provenance analysis using detrital zircons to infer compressional setting in Yukon during the Triassic. The geodynamic and basin setting during the deposition of the Montney Formation thus becomes an issue (Ferri and Zonneveld, 2008). Recent provenance analyses using detrital zircon of Triassic sedimentary rocks in British Columbia and Alberta indicate an active sedimentary source to the west (Golding et al., 2016), providing additional evidence to support a westward emerging land (Tozer, 1982; Gibson and Barclay, 1989). Nevertheless, it is still unclear whether the Triassic succession, including the Montney Fm., was deposited in an early retro-foreland setting, as the Jurassic setting, or pro-foreland setting, or even during a renewed rapid extensional event in a back-arc setting along the inherited Paleozoic passive margin. A fundamental difference between these types of basins is that the subsidence evolution shows uniqueness in its temporal and spatial trends (Fig. 1, e.g. Naylor and Sinclair, 2008; Sinclair and Naylor, 2012 and references herein). For example, additional accommodation to flexural tectonics may be created by the superimposed effects of dynamic subsidence in retro-foreland (slab-related), a mechanism not possible in pro-foreland basins (Fig. 1). Likewise, passive margin and back-arc setting are primarily dominated by increasing subsidence when going seaward in response to thermal cooling and no processes could account for an entire inversion and uplift of the most distal environments (Fig. 1).

Detailed subsidence analyses have been published for the early stage of the WSCB basin evolution, thus illustrating its thermal subsidence dynamics during the Early Paleozoic (Bond and Kominz 1984). The subsidence evolution of the Jurassic collisional foreland basin has also been addressed and characterized in several

studies (Price, 1994; McCartney, 2012). However, the subsidence dynamic of the Triassic in the WCSB has not previously been characterized. Here, we present subsidence analyses using a backstripping method integrating recent high-resolution stratigraphic correlations for the Montney Formation (Crombez, 2016; Crombez et al., 2016; Euzen et al., this volume). Backstripping the sediment and water fill allows the effects of sediment and water loading to be quantitatively determined, thus isolating the remaining effect of the tectonic driving forces (Watts and Ryan, 1976). We backstripped six wells and two outcrop sections along a proximal to distal transect (approx. NE to SW) to quantify the spatial and temporal evolution of the subsidence during deposition of the Montney Fm.. In order to constrain the driving forces for subsidence, the overall basin evolution, from the Early Paleozoic to recent, was taken into account. Subsequently, we analyzed the entire backstripped subsidence to quantify the relative influence of thermal, flexure and sediment loading. Sediment fluxes were also discussed using solid siliciclastic accumulation rates to constrain uplift dynamics. Finally, by integrating the proposed evolution into the evolution of the Canadian Cordillera, we can discuss a geological scenario to constrain the geodynamic evolution during Montney Formation deposition.

DATA AND METHOD

The tectonic subsidence curves were generated using GENEX software for six subsurface wells and two outcrop sections (Fig.2, Table 1). These curves document basin dynamics during Montney Formation deposition. GENEX is a numerical simulation program developed by IFPEN (IFP Energies nouvelles) during the 1980's that integrates subsidence, thermal and pressure reconstruction, maturity and compositional petroleum generation and expulsion. The full

workflow and concepts in GENEX to backstrip wells, have been detailed in Ungerer et al. (1990) and Forbes et al. (1991). GENEX has been widely used in various types of basin and petroleum systems (Faure et al., 2004; Rudkiewicz et al., 2007; Rohais and Moretti, 2017). In the present study, we took benefit of the work of Ness (2001) that already carried out 1D basin analysis on sixteen wells in the WCSB to understand when hydrocarbons in WCSB Triassic reservoirs were generated and expelled from their sources. By matching burial and thermal history with available vitrinite reflectance datasets, Tmax (determined by Rock-Eval pyrolysis), bottom-hole temperatures, pressure profiles, and apatite fission track analyses, Ness (1991) achieved a well-constrained basin analysis and restored a geologically reasonable basin dynamic scenario. Based on the work of Ness (1991), we used here a selection of six wells (Table 1) from the westernmost part of the WCSB (autochthonous foreland) and adjacent allochthonous units of the foreland-and-thrust belts and processed these wells in GENEX to compute the tectonic subsidence.

Total subsidence and tectonic subsidence after sediment decompaction were restored through time, by integrating porosity-to-depth laws for each lithology, paleobathymetry, eustatic variations and erosion values (Airy type model such as in Steckler and Watts (1978)). The paleobathymetry values are derived from geometrical restorations based on sedimentological and sequence stratigraphy studies (Crombez, 2016; Crombez et al., 2016). The most important source of error when backstripping well sections is uncertainty in paleobathymetry. Thus, we chose to explore a large range in paleobathymetry (+/- 50% of the mean estimated paleo-water depth value, see Table 1).

To discuss the potential influence of post-rift thermal subsidence, we estimated the stretching with the Beta factor (ß) (i.e. ratio between the initial crustal and the final crustal thickness; McKenzie, 1978) using the Lithoprobe section interpreted by Monger and Price (2002) that is presented in Fig. 2. The values are presented in Table 1.

The full data set for backstripping is available as supplementary material in the appendix (two outcrop sections and six wells). Fig.3 presents the formations and their tops, the groups derived from the Alberta Geological Survey (2015) and the age model used for the present study. Ages were adjusted using the most recent reference (Cohen et al., 2013 updated). Triassic and Montney tops (Fig. 4) have been updated using recent stratigraphic correlations (Crombez, 2016).

The stratigraphic architecture contains an indirect, yet quantifiable, record of regional uplift that is the sediment supply. Indeed, sediment supply through time can be related to uplift and denudation of the sediment source regions (e.g. Bonnet and Crave, 2003; Rohais et al., 2012). Likewise, we extracted from the modeled wells and outcrops solid (porosity corrected) sedimentation rates (m/Myr) resulting from the siliciclastic component (sandstone, siltstone, shale) that can be discussed in terms of sediment supply dynamics. These values are directly available from the GENEX results.

GEOLOGICAL SETTING

THE CORDILLERA: TERRANES, BELTS AND EVOLUTION

The Canadian segment of the Cordillera is commonly subdivided into five approximately N-S belts (Fig.2, e.g. Coney et al., 1980). Each belt is oriented parallel to the overall tectonic trend and has been identified by its distinctive

bedrock geology, ages, physiography, metallogeny and deep-seismic expression (Fig.2) (Wheeler and Gabrielse, 1972; Monger et al., 1972, 1982; Tipper et al., 1981; Gabrielse et al., 1991; Hammer and Clowes, 1997; Clowes et al., 2002). These belts correspond to two superterranes (Insular and Intermontane), two intervening swaths of dominantly plutonic and metamorphic rocks (Omineca belt and Coast belt), and the easternmost retro-foreland belt (including the WCSB) that overlies and thins over the stable North American craton (Fig. 2).

The Intermontane superterrane includes from west to east the Stikinia (ST), Cache Creek (CC), Quesnellia (Q), Yukon-Tanana (YT) and Slide Mountain (SM) terranes (Fig. 2). The Omineca belt corresponds to the suture zone between the Intermontane superterrane and the North American ancestral craton (Price, 1994). Over much of its length, the Omineca belt is bounded both side by fold-and-thrust belts (Fig. 2). The Yukon-Tanana and Quesnellia terranes were connected during Mid-Paleozoic times (Murphy et al., 2006; Nelson et al., 2006; Colpron and Nelson, 2009; Beranek and Mortensen, 2011).

The timing of terrane amalgamation, as well as the timing of accretion of the resulting superterrane to the western margin of ancestral North America in Canada are still debated, but the most recent works provide a well-constrained and consistent geological scenario that is briefly summarized hereafter.

The Yukon-Tanana terrane detached from western ancestral North America during the latest Devonian to Early Mississippian initiation and growth of the Slide Mountain Ocean (e.g. Mihalynuk et al., 1999; Nelson et al., 2006; Colpron and Nelson, 2009; Beranek and Mortensen, 2011), in response to rollback of the downgoing slab generating an extending back-arc region (Gabrielse, 1991; Piercey et al., 2004). Persistent east-dipping subduction and expansion of the Slide

Mountain ocean were documented from Early Mississippian to Early Permian time (e.g. Nelson et al., 2006; Colpron and Nelson, 2009; Beranek and Mortensen, 2011). By the Early to Middle Permian, the geodynamic setting changed when the polarity of subduction reversed below the Yukon-Tanana terrane, and Slide Mountain ocean lithosphere began to be consumed (Murphy et al., 2006; Nelson et al., 2006; Beranek and Mortensen, 2011). The causal factor of subduction reversal during the Permian remains unknown. A fore-arc setting associated with a Late Permian west-dipping subduction is indicated by the presence of arc magmatic, blueschist and eclogite clasts along the eastern part of the Yukon-Tanana terrane (Mortensen et al., 1999). Evidence indicates that arc-continent collision, and accretion of the Yukon-Tanana terrane along the ancestral North American continental margin, occurred during Late Permian (Beranek and Mortensen, 2011). East verging structures of latest Permian to earliest Triassic age have also been described in the Slide Mountain terrane (Monger et al., 1991; Saleeby and Busby-Spera, 1992). The timing for its thrusting was constrained by Late Permian intrusives which cross-cut the bounding thrust fault in British Columbia (Harms, 1985; Gabrielse et al., 1993). This suggests that the Slide Mountain terrane most likely accreted to the autochthon during the Late Permian-Early Triassic (Beranek and Mortensen, 2011), earlier than the commonly inferred Middle Jurassic obduction age for Slide Mountain oceanic crust (e.g. Harms, 1989; Struik et al., 1992, Murphy et al., 1995; Ferri, 1997; Ash, 2001). This event in the Canadian Cordillera occurred approximately synchronous with the Sonoma orogeny (Siberling, 1973) in the US Cordillera (Mortensen et al., 2007).

Geological thought on the Mesozoic-Cenozoic evolution of the Canadian Cordillera has traditionally invoked accretion of island arcs, and their related basement terranes to the western ancestral North America continental margin

(Monger et al., 1982, 1991; Mihalynuk et al., 1992; 1994; Ash, 2001). In these terrane accretion models, the Cache Creek terrane is interpreted as a composite of Late Triassic accretionary prisms or subduction-related accretionary complex associated with the Stikinia terrane, generated by Middle Triassic to Early Jurassic destruction of the late Paleozoic ocean lithosphere (Cache Creek, e.g. Colpron et al., 2015). Upper Paleozoic seamounts preserved in the Cache Creek terrane indicate that it originated on the opposite side of Panthalassa from the Cordilleran accretionary orogeny (Monger and Ross, 1971; Johnson and Borel, 2007). In the late Rhaetian (late Triassic), renewed subduction beneath Stikinia was indicated by sedimentary deposits in British Columbia (e.g. Barresi et al., 2015) and emplacement of ca. 204–195 Ma plutons (Rhaetian-Sinemurian, Colpron et al., 2015). At that time, subduction is inferred to have occurred on both sides of Stikinia (ST) (Marsden and Thorkelson, 1992). The main east-dipping subduction along the entire western margin of Ancestral North America was thus re-established by the Middle to Late Triassic (Ferri, 1997; Colpron and Nelson 2009). Crustal thickening, followed by regional exhumation of the Yukon-Tanana terrane, suggests that convergence and thrusting between Stikinia, Cache Creek, Quesnellia, and the North American margin had begun by the Sinemurian–Pliensbachian (Early Jurassic, Colpron et al., 2015). The northern Whitehorse Trough in the Yukon is thus interpreted to be a piggyback or wedge-top basin during the initial stages of development of the northern Cordilleran orogeny (Early Jurassic, Colpron et al., 2015).

The model presented herein has strong geodynamic implications. Assuming a wide Slide Mountain ocean, such a model infers transition from a west-dipping subduction (back-arc closure of the Slide Mountain ocean), slab detachment, and east-dipping subduction from the Late Permian to the Late Triassic (e.g. Ferri,

1997; Tardy et al., 2003), a time slot earlier than the Jurassic foreland evolution. Assuming a narrow Slide Mountain ocean back-arc, a simple shortening by imbrication would have been enough to consume the oceanic crust, associated with a main "stable" east-dipping subduction.

By the Early to Middle Jurassic, the Insular Terrane was interacting with western North America (McClelland and Gehrels, 1990; van der Heyden, 1992), and a Cordillera-long continental arc developed (Gehrels et al., 2009) with a tectonic regime that persisted until the early Cenozoic. The growth of the Cordilleran orogeny was then accompanied by the development of Western Canada Sedimentary Basin (collisional retro-foreland).

WESTERN CANADA SEDIMENTARY BASIN

The Western Canada Sedimentary Basin (WCSB) forms a very large sedimentary wedge over Precambrian crystalline basement (Fig. 2). This wedge has a maximum thickness of about 5,500 m along the edge of the Rocky Mountain Foothills, and thins northeastward to a zero-edge along the basin margin. It includes the Alberta Basin and the Williston Basin, which are separated by the Sweetgrass Arch (Fig. 2).

Architecture of the "Paleozoic miogeocline-platform"

The western margin of the WCSB, now preserved in the Cordillera, has had a long tectonic history dominated by major episodes of extension from the Proterozoic to the Paleozoic (Fig. 3). Two km-thick Proterozoic to Cambrian sequences in the Cordilleran fold-and-thrust belt are generally absent in the undeformed WCSB to the east. These sequences record two proterozoic stages of continental rifting and extension around 1500-1400 Ma and 770-730 Ma (Hein and McMechan, 1994). An age of 555 to 600 Ma (Neo-Proterozoic) for the breakup of the continental

ancestral North American craton and initiation of drift along the early Paleozoic passive margin has been established using the tectonic subsidence backstripping method (Bond and Kominz, 1984). Following a long period characterized mainly by erosion / non-deposition in the WCSB, sedimentation resumed during the Devonian.

The Devonian (Granite Wash, Slave Point, Beaverhill Lake-BHL, Duvernay, Ireton, Winterburn, Wabamun and lower Exshaw Formations) was deposited primarily within a carbonate platform setting facing open marine conditions to the west (see Mossop and Shetsen, 1994 and reference herein). The Devonian-Carboniferous boundary occurs in the black shale of the lower Exshaw and Bakken Formations (Fig. 3).

The Carboniferous (upper Exshaw / Bakken, Banff, Rundle Group, Golata, Kiskatinaw, Taylor Flat, Ksituan Formations) includes proximal carbonate platforms and ramps, and sandstone-dominated siliciclastic facies that were deposited in slope to continental settings, as well as to basinward shale, spiculite and bedded chert of basin to slope origin (Barclay et al., 1990; Richards et al., 1994). Active extensional tectonism with high subsidence rates are documented in the Peace River Embayment area as well as in the Prophet Trough (e.g. O'Connell, 1990; Barclay et al., 1990).

The Permian (Belloy and Fantasque formations) consists mainly of marine siliciclastics and silty to sandy carbonates that are commonly silicified (Henderson, 1989; Henderson et al., 1994). Deposits are relatively thin and preserved only in a narrow belt throughout most of the eastern Cordillera fold-and-thrust belt and, locally, on the Interior Platform in the Peace River area. Thicker deposits are preserved in the Ishbel Trough, which corresponds to an extensive structure

developed on the down-warped and down-faulted ancestral western margin of the North American plate (Fig. 2; Henderson et al., 1994). Numerous lines of field evidence including geological mapping, biostratigraphic and diagenetic studies, structural analysis suggest active tectonism during sedimentation and a potential compressive setting with a large peripheral bulge (e.g. Fossenier, 2002; Henderson et al., 2010; Zubin-Stathopoulos et al., 2011).

Jurassic to Eocene foreland stage

The classic indicators of foreland basin initiation such as basin geometry, depositional setting, subsidence backstripping results and sedimentary provenance suggest that the collisional retro-foreland phase began during the Mid- to Late Jurassic (e.g. Poulton, 1989; Gillespie and Heller, 1995; Fuentes et al., 2009; McCartney, 2012). The foreland phase then culminated in the Middle Eocene at the end of the Laramide Orogeny. Using subsidence backstripping, McCartney (2012) proposed that the basal series (Sinemurian–Toarcian, Nordegg Fm.) of the Fernie Fm. was deposited in a backbulge depozone (sensus DeCelles and Giles, 1996) and thus record initial low subsidence related to earliest development of the foreland phase (Fig. 3). Eastward migration of the forebulge occurred during the Middle Jurassic as recorded by the sub–upper Fernie unconformity (Oxfordian–Kimmeridgian; Poulton, 1989). During the Kimmeridgian, the upper Fernie Fm. (Nikanassin Fm.) was deposited in a rapidly subsiding foredeep that received the first influx of westerly-derived detritus from the Cordilleran orogen (Poulton, 1989). These formations are mainly fluvial, deltaic and shallow marine siliciclastics to fine-grained condensed and starved shelf successions (Poulton et al., 1994).

The Cretaceous (Cadomin, Bluesky/Gething, Wilrich, Falher, Notikewin, Harmon, Cadotte, Paddy, Shaffesbury, Dunvegan, Kaskapau, Cardium, Muskiki, Marshybank, Puskwaskau and Wapiti formations) was dominated by conglomeratic to fine-grained siliclastic deposits derived primarily from the rising Cordillera to the west and deposited within the retro-foreland basin (see Mossop and Shetsen, 1994).

STRATIGRAPHIC ARCHITECTURE OF THE WCSB TRIASSIC SERIES AND MONTNEY FM.

WCSB triassic stratigraphy and nomenclature (Fig. 4) are mainly based on McLearn and Kindle (1950), Hunt and Ratcliffe (1959), Armitage (1962), Barss et al. (1964), Stewart (1984), Tozer (1984), Gibson and Barclay (1989), Gibson and Edwards (1990a, b), Glass (1990) and many others. In the British Columbia foothills outcrop belt, Triassic rocks are subdivided into the Grayling, Toad, Liard, Charlie Lake, Baldonnel, Pardonet and Bocock formations (Edwards et al., 1994). In the subsurface of the Peace River area, six main formations are present (Fig. 4). In ascending order these are the Montney, Doig, Halfway, Charlie Lake, Baldonnel, and Pardonet formations.

The main unconformities are located at the base of the Triassic (Permian-Triassic Unconformity), at the base of the Doig/Halfway cycle (Sequence Boundary SB4, Barss et al., 1964, Crombez 2016; Crombez et al., 2016), within the middle Charlie Lake Fm. (Coplin Unconformity; Aukes and Webb, 1986; Campbell et al., 1989), and at the top of the Triassic with the sub-Jurassic Erosion (Fig. 4).

The Montney Fm. consists primarily of fine-grained dolomitic sandstone and siltstone with subordinate amounts of shale and a moderate to low clay content,

locally high organic content (Davies, 1997; Zonneveld et al., 2010; Chalmers and Bustin, 2012; Crombez, 2016). Recent biostratigraphic works (Orchard and Zonneveld, 2009; Golding et al., 2014a, 2014b, 2015, 2016) indicate that the Montney Fm. is early Triassic in age. Three main sequences have been recognized in the Montney Fm., with proximal to distal settings (e.g. Davies et al., 1997; Zonneveld et al., 2011; Crombez, 2016; Crombez et al., 2016). These sequences are organized in complete second order cycles with sequence 1, 2 and 3 corresponding to Transgressive System Tract (TST), Highstand System Tract (HST) and Falling Stage to Lowstand System Tract (FSST/LST) like packages respectively (Fig. 4). Biostratigraphic data (Orchard and Zonneveld, 2009; Golding et al., 2014a, 2014b, 2015, 2016) were integrated into the most recent stratigraphic architecture subdivision (e.g. Crombez, 2016) and indicate that the boundary between sequences 1 and 2 is close to the Induan-Olenekian boundary (SB2), and the boundary between sequence 2 and 3 corresponds to the Smithian-Spathian boundary (SB3). The top of the Montney Fm. relates to earliest Anisian times (Fig. 4).

The Montney Fm. reaches a maximum thickness of ca. 350m in British Columbia and thins toward the eastern subcrop edge (Fig. 5). Detailed sequence analysis (Crombez, 2016) shows that each individual third order sequence can reach a maximum thickness close to 225m and that the depocenters of these sequences moved toward the west suggesting a filling of the basin primarily by eastern sources (Fig. 6). Regarding the paleobathymetry, Crombez et al. (2016) and Crombez (2016) suggest that the deposition of the Montney Fm. took place on a shelf rather than in a deep abyssal basin (bathymetry < 250m, Table 1).

SUBSIDENCE AND BASIN DEFORMATION

TRIASSIC DYNAMICS

Results

Along the ca. 500-km long proximal to distal transect, we used tops derived from our high resolution stratigraphic correlations (Crombez, 2016; Crombez et al., 2016) to compute tectonic subsidence for the six wells and two outcrop sections (Fig. 7). Average, minimum and maximum subsidence rate during the deposition of the Montney Fm. for each sequence are spatially presented in Fig. 8. Solid (porosity corrected) siliciclastic sedimentation rates were quantified to evaluate the sediment supply dynamic (Fig. 9).

Late Permian (Belloy and Fantasque formations) was characterized by very low tectonic subsidence as well as minor local uplift in comparison with preceding Carboniferous times (Fig. 7). The Permian-Triassic unconformity recorded the initiation of tectonic subsidence and basin margin tilting with up to 100-110 m/Myr of tectonic subsidence in the deepest part of the basin (sections #1 and 2, see Table 1 and Fig. 2 for location) and 5-10 m/Myr along the basin edge (wells #7 and 8) (Fig. 7). Sequence 1 (252-249.7 Ma) was then characterized by decreasing tectonic subsidence in comparison with Late Permian-Earliest Triassic (Fig. 8), from ca. 25-30 m/Myr in the deepest part of the basin (sections #1 and 2), to ca. 50 m/Myr in the main depocentre (well #4) and ca. 15-20 m/Myr along the basin edge (wells #6, 7 and 8). It indicates an overall westward tilting of the basin superimposed with maximal tectonic subsidence localized in the main depocentre east to the present day limit of the fold-and-thrust belt. Sediment supply was relatively low and increased rapidly after sequence 1 (Fig.9).

Sequence 2 (249.7-248 Ma) was characterized by tectonic inversion with evidence of uplift in the western (deepest) part of the basin (Fig. 8; sections #1 and 2). A

subsiding depocentre (ca. 10-20 m/Myr) was localized in the vicinity of wells #5 to #6 (Fig. 7, Fig. 8). Sequence 3 (248-247 Ma) was characterized by the same trend initiated during deposition of Sequence 2 (Fig. 7, Fig. 8). The subsiding depocentre (wells #5 to 6) was then characterized by very low tectonic subsidence rates, ca. 2-5 m/Myr (Fig.8). The uplift trends steadied along the basin eastern edge and coevally, sediment supply increased to reach its maximum of the Triassic times (Fig. 9).

During the development of sequence boundary SB4 (i.e. Montney-Doig contact), the entire basin was uplifted (Fig. 8). The entire basin was then characterized by very low tectonic subsidence during the Middle Triassic (Fig. 7). A second pulse, less intense than during SB4, of increasing sediment supply was recorded up to the Coplin unconformity (Fig. 9).

During the Triassic, sediment supply was characterized by a rapid (ca. 2-6 Myr-long) increase (Sequence 1, 2 and 3) followed by a progressive (ca. 20-30 Myr-long) decrease down to very low value during the Late Triassic (Fig. 9). Two pulses can be identified within this Triassic-scale trend, with the first one (Sequence 1 to 3, Montney Fm.) corresponding to a maximum, and a second one (approximately Middle Triassic prior to the Coplin Unconformity) recording a more gentle sediment supply increase (Fig. 9). These two pulses are separated by a major unconformity (SB4), followed by a sharp decrease of the sediment supply (corresponding to the basal Doig Fm.).

Interpretation

The tectonic subsidence evolution with basin margin tilting, early inversion of the deepest part of the basin (West) and landward migration of subsiding depocentres share many similarities with the dynamic of a foreland basin and its

four discrete depozones (Fig. 1; wedge-top: WT, foredeep: FD, forebulge: FB and backbulge: BB, *sensu* DeCelles and Giles, 1996).

The deepest part of the basin (section #1) was characterized by the most distal and starved depositional systems and was the first to be inverted following overall tilting (Fig. 7). The initial overall basin tilting may be interpreted as a flexure of the basin margin in response to tectonic loading. As the section #1 is mainly characterized by starved and distal deposits, the uplift trend initiated at the transition between sequences 1 and 2 could have occurred in the wedge-top or forebulge (*sensu* DeCelles and Giles, 1996). The section #1 records continuous deposition from the Late Permian into the Early Triassic (Henderson, 2011). This section was located on the down-faulted eastern margin of the Prophet Ishbel Trough (Fig. 2; Henderson et al., 2012). A wedge-top setting would imply that the Prophet Ishbel Trough was fully filled at the end of the Permian, inverted and back-thrusted in front of the Kootenay terrane (Fig. 2) to form a wedge-top during the Triassic. Although inversion was documented (Henderson et al., 2010), the preserved Permian facies support neither an overfilled configuration (Henderson et al., 2012), nor an important tectonic uplift of the trough at the end of the Permian. Additionally, the subsidence rates from section #1 to well #3 suggest that this entire region evolved as a whole from sequence 1 to 3 (Fig. 8). Consequently, the most likely interpretation is that Ursula Creek was sitting on the edge of a large peripheral forebulge and the entire WCSB interpreted as backbulge basin during the Triassic. The forebulge to backbulge area could then be fault-bounded, as shown by Henderson et al. (2012) and Zonneveld et al. (2011), hosting half graben-like structures similar to the Karoo foreland basin of Africa (Catuneanu, 2004).

The eastward migration of the subsiding depocentre from sequence 1 to 3 can be interpreted as a backbulge to forebulge migration with the eastern edge of the forebulge initially localized at the present day transition between the fold-and-thrust belt and the undeformed WCSB (well #3). The tectonic subsidence evolution during SB4 and the Middle Triassic suggests that the entire WCSB behaved as a large and slowly subsiding basin just prior to the Coplin unconformity (Fig. 7). Following the Coplin unconformity, a renewal of tectonic subsidence associated with new basin margin tilting was then recorded during Late Triassic (Fig. 7).

Sediment supply dynamics during the Triassic also supports a major uplift in the catchment area, potentially related to overall basin margin tilting during the Permian-Triassic boundary (Fig. 9). The progressive decrease of sediment supply suggests that the uplift rate in the catchments was not permanent but transient at the scale of the Triassic (Rohais et al., 2012). The decrease in sediment supply following SB4 could correspond to a re-adjustment in the catchment potentially related to backbulge - forebulge inboard migration.

The tectonic subsidence values quantified in the subsidence backstripping are strongly dependent on paleobathymetry estimations. However, error bars on Figure 8 show that uncertainties on paleobathymetry do not affect significantly the overall trends and basin dynamic proposed in this study.

INTEGRATION WITHIN WSCB EVOLUTION

To constrain the driving forces for subsidence as well as to define the main depozones during the deposition of the Montney Fm., the overall basin evolution from the Early Paleozoic to Recent needed to be taken into account. We computed the entire backstripped subsidence for the six wells and two outcrop

sections (Fig. 10) to quantify the relative influence of thermal, flexure and sediment loading-induced subsidence. Additionally, sediment fluxes were also analyzed using solid siliciclastic sedimentation rates to constrain uplift dynamics.

Key pre-Triassic events

The very first Mid-Ocean Ridge basalt (MORB) evidence in the Slide Mountain ocean (SM) occurred during Cycle II of Nelson et al. (2006), ca. 365-357 Ma (Late Devonian-Earliest Mississippian). The backstripped tectonic subsidence curves that we calculated were then compared with post-rift tectonic subsidence curves initiated at 365 Ma (Fig. 10) and calculated from the stretching model of McKenzie (1978) for different amounts of stretching, using the beta stretching values defined from the Lithoprobe cross-section results (Table 1). There is a very good match for all the backstripped curves with the theoretical post-rift tectonic subsidence evolution from 365 Ma to ca. 320-330 Ma (end Mississippian-Pennsylvanian boundary). We thus propose that thermal processes typical of a passive margin evolution mainly controlled tectonic subsidence during the Latest Devonian to Mississippian. Subsequently, all of the wells and sections included herein indicate a deficit in cumulative tectonic subsidence compared to the thermal model (Fig. 10), suggesting that the driving forces controlling thermal subsidence were no longer active during the Carboniferous. This interpretation is consistent with Cycle V of Nelson et al. (2006), ca. 314-269 Ma (Pennsylvanian-Early Permian) that recorded the fore-arc initiation on the eastern part of the Yukon-Tanana terrane (Klinkit arc). Potentially, the Devonian slab retreat stopped in response to the over-steepening of the subducted slab, to a slab break-off or even to an arc-arc collision. From ca. 300 Ma to 252 Ma (Permian), the most inboard wells (#5, 6, 7 and 8) were gently uplifted, while the most distal ones

were characterized by very low tectonic subsidence (Fig. 10). Combined with sedimentological evidence such as the sediment provenance and the distribution of depositional environments (Richards et al., 1994; Henderson et al., 1994), this suggests a forebulge to backbulge dynamic, which is very consistent with the paleogeographic reconstruction for Late Carboniferous and Permian with a narrow and very deep Prophet Trough, Ishbel Trough, their associated peripheral bulges and poorly preserved backbulge deposits (Henderson et al., 2010, 2012; Zubin-Stathopoulos et al., 2011). Consequently, it is clear that the very oldest deposits of the Montney Fm. were deposited in a peripheral forebulge to backbulge setting in the WCSB.

Key post-Triassic events

The Late Triassic was characterized by low tectonic subsidence rates (Fig. 7, Fig. 10). The hinge line between subsiding versus uplifted depozones occurred between wells #5 and #6 as well as uplifted zones in the deepest part of the basin (section #1, Fig. 10). The basin was sediment-starved and/or fully bypassed as indicated by a very low sediment accumulation rate (Fig. 9). Depositional systems summarized by Gibson and Barclay (1989), Gibson (1993) and Edwards et al. (1994) consist of restricted and protected settings throughout the WCSB, mainly shallow marine environments across the previously identified peripheral forebulge and open marine setting to the west. The paleogeography of Late Triassic, combined with the spatial and temporal evolution of tectonic subsidence, are consistent with a late underfilled stage to early filled stage in the evolution of a foreland system, with temporary dominance of flexural tectonics such as in the Karoo model of Catuneanu (2004).

During the Early Jurassic, prevailing low tectonic subsidence rates (Fig. 10), and paleogeographic restoration suggest a peripheral forebulge to backbulge setting for the WCSB. The hinge line between subsiding versus uplifted depozones was localized between wells #3 and #4 (Fig.10). The Late Jurassic (ca. 145-150 Ma) recorded the rapid increase of tectonic subsidence in the deepest part of the WCSB (section #1 to well #3), combined with a slowly subsiding depozone (wells #4 to #6) and an uplifted depozone inboard (wells #7 and #8) (Fig. 10). This can be interpreted as a foredeep - forebulge inboard migration during Late Jurassic. In this framework, Lower to Middle Jurassic can also be interpreted as forebulge – backbulge inboard migration. Amplitude, timing and basin-scale distribution of tectonic subsidence during early collisional retro-foreland evolution (Late Jurassic-Early Cretaceous) are very similar with Triassic trends (Fig. 10). The tilting of the margin, followed by pulse of uplift during Late Jurassic to Early Cretaceous can be interpreted as early, underfilled to filled phases of foreland basin evolution *sensu* Catuneanu (2004). The relative balance between dynamic subsidence and flexure may account for such an evolution. It implies that the “true foredeep” inboard migration and arrival in the WCSB occurred at ca. 110-120 Ma (possibly the sub-Cadomin).

During the Cretaceous and Cenozoic, the WCSB was characterized by a typical forebulge – foredeep – fold-and-thrust belt evolution (McCartney, 2012; Pana and van der Pluijm, 2015) with a final isostatic rebound (Fig. 10). Several pulses within the backstripped subsidence curves can be correlated with the well-known terrane accretion in the North American Cordillera orogen (Pana and van der Pluijm, 2015).

DISCUSSION

STRUCTURAL SETTING OF THE MONTNEY FM.: EXTENSION VERSUS COMPRESSION

Field and analytical studies including geological mapping, structural studies, tectonostratigraphic analysis, U-Pb zircon dating and detrital zircon studies in western Canada have reported compelling evidence for Late Permian-Early Triassic (ca. 250 Ma) collision (e.g. Mortensen et al., 2007; Beranek and Mortensen, 2011; Henderson et al., 2012). The accretion of terranes is well documented from Early to Middle Jurassic time because intense deformation and stitching plutons of that age occur in the southern Canadian Cordillera (e.g. Gabrielse and Yorath, 1989; Murphy et al., 1995). Therefore; the Triassic period should thus be viewed as part of an overall compressive setting continuum, or conversely as part of renewed extension within a back-arc system. Reactivation of inherited extensional structures is documented during the Triassic (Cant, 1986; Edwards et al., 1994; Zonneveld et al., 2011), however driving forces were neither documented nor quantified in these studies with investigated backstripped wells and outcrop sections.

The spatial and temporal evolution of backstripped tectonic subsidence (Figs. 7, 8, and 10) during the Triassic can be interpreted as a continuum evolving from (1) Late Permian: a narrow foredeep, peripheral forebulge, and associated backbulge with poorly preserved deposits, diagnostic of an early underfilled stage of foreland basin evolution where flexural uplift overtakes dynamic subsidence, to (2) Early Triassic (Montney Fm.): a foredeep – forebulge – backbulge with thick clastic deposits diagnostic of a late underfilled stage of foreland basin evolution where dynamic subsidence overtakes flexural uplift, to finally (3) Middle to Late Triassic: a forebulge – backbulge configuration with shallow marine to restricted deposits across the entire WCSB, diagnostic of an early filled phase during which

dynamic subsidence overtook flexural uplift but progressively decreased, as suggested by the overall uplift of the forebulge depozone. In this context, extensional faulting is interpreted as local rejuvenation of inherited structures across a large forebulge flexure, as well documented in other foreland basins (e.g. Karoo foreland basin of Africa; Catuneanu, 2004).

GEODYNAMIC SETTING OF THE MONTNEY FM.: RETRO-FORELAND BASIN VERSUS COLLISIONAL PRO-FORELAND BASIN

Several works suggest that subsidence rates from the sedimentary record within foreland basins may be key for differentiating the type of foreland basin (Fig. 1; DeCelles and Giles, 1996; Ziegler et al., 2002; Sinclair and Naylor, 2012). As previously discussed, the Montney Fm. can be considered to be a textbook example that records the entire basin evolution from the earliest underfilled to the intermediate filled stage of foreland basin evolution. The configuration of the basin during Late Carboniferous to Permian (narrow and deep foredeep, important forebulge erosion, poorly preserved backbulge), combined with the subsidence evolution presented in this work, indicate that this period of time was characterized primarily by a flexural uplift that overtook dynamic subsidence, if any dynamic subsidence occurred. Collisional pro-forelands lack a mechanism for dynamic subsidence (DeCelles and Giles, 1996; Ziegler et al., 2002), so we propose that the Late Carboniferous to Permian period was characterized by a collisional pro-foreland setting.

Furthermore, we show spatial and temporal subsidence changes that suggest dynamic subsidence during deposition of the Montney Fm. The trends presented and discussed in our study are valid even using the lowest estimations for paleobathymetry (Fig. 8). Additional flexure in retro-foreland basins is caused by

dynamic subsidence induced by the subducting slab (Beaumont, 1981; DeCelles and Giles, 1996). Thus, we proposed that the Early Triassic (Montney Fm.) was deposited in a retro-foreland basin setting. Data from worldwide foreland basins suggest that forebulge and backbulge depozones are best preserved in retro-arc settings (Catuneanu, 2004; DeCelles, 2012), which renders our interpretation even more consistent. A retro-foreland setting is also inferred for the Jurassic-Cretaceous western Canadian foreland basin.

Following the Late Permian, which is characterized by the lack of eastward subduction on the western part of the Yukon-Tanana and Quesnellia terranes and the shortening of the Slide Mountain ocean by imbrication or west-dipping subduction (e.g. Ferri, 1997; Nelson et al., 2006), the Montney Fm. recorded the reactivation of eastward subduction below the ancestral North American craton. The size and configuration of the Slide Mountain ocean have been the subject of much discussion, probably because of its south to north gradient from marginal sea to large oceanic basin merging together with others oceans to the North (Shephard et al., 2013). Assuming a large ca. 1300 to 3000 km-wide Slide Mountain ocean (e.g. Snyder and Brueckner 1985; Nokleberg et al., 2000; Nelson et al., 2006), only west-dipping subduction could have consumed the ocean during the Late Permian. This interpretation is supported by direct evidences for an active west-dipping subduction during the Late Permian found in blueschist and eclogite rocks in the Anvil Allocththon in the southern Yukon (Erdmer, 1987; Erdmer and Armstrong 1988). As we demonstrate the occurrence of an east-dipping subduction below the WCSB during Early Triassic, this suggests a potential slab break-off and related isostatic rebound to have occurred during Late Permian – earliest Triassic transition. Nevertheless, the north to south extension of the Late Permian west-dipping subduction can be debated since the lack of high-

pressure assemblages elsewhere in the Cordillera suggests that Slide Mountain ocean shortening may have occurred without substantial subduction (Ferri, 1997).

WIDER IMPLICATIONS FOR CORDILLERA EVOLUTION

The main east-dipping subduction along the entire western margin of Ancestral North America was re-established as early as Middle to Late Triassic based on volcanic-arc assemblages in Quesnellia terrane (Monger et al., 1991; Ferri, 1997; Colpron and Nelson 2009). Thus, our findings suggest an earlier timing than Jura-Cretaceous, or possibly an additional event, during the birth of the North American Cordilleran orogen. The simplest interpretation would be to propose a lag time (ca. 5-10 Myr) between evidence for subduction activity recorded in the dynamic subsidence of a retro-foreland basin versus volcanic-arc emplacement.

We also show that the evolution of the WCSB from the Early Triassic (Montney Fm.) to the Middle and Late Triassic did not follow the traditional backbulge – forebulge - foredeep sequence. Conversely, the Middle to Late Triassic was characterized in the WCSB by uplift and large scale flexure. This suggests that dynamic subsidence did not drive tectonic subsidence anymore, which could be interpreted in terms of decreasing influence of underlying slab forces. This interpretation is corroborated by the end of activity of the east-dipping subduction in the late Triassic, followed by the entrapment and final collapse of the Cache Creek terrane between Quesnellia and Stikinia terranes (Mihalynuk et al., 1994; Colpron et al., 2015). During the latest Triassic, renewed east-dipping subduction beneath Stikinia was recorded by sedimentary deposits (e.g. Barresi et al., 2015) and emplacement of ca. 204–195 Ma plutons (Marsden and Thorkelson, 1992). Subsequent exhumation was recorded in the Yukon Territory (Early Jurassic; Colpron et al., 2015) that may correspond to isostatic rebound induced

by slab break-off of the Cache Creek terrane. Basins, such as the Whitehorse Trough, were characterized by rapid subsidence that was initiated in the Sinemurian (Early Jurassic), and therefore may be interpreted as wedge-top depozones recording some of the early stages of development of the North America Cordilleran orogeny (Colpron et al., 2015).

The backstripped subsidence curves of the WCSB (Fig. 10) provide a record of the evolution of the entire northern Cordillera, from its Cambrian-Silurian rifting, passive margin (Fig. 11-a and 11-b) and Devonian back-arc development (Fig. 11-c) through three distinct foreland stages resulting in the final orogeny (Fig. 11-d to 11-j) that is consistent with the most recent advances in the understanding of the Cordilleran orogeny (e.g. Monger and Price, 2002; Nelson et al., 2006; Murphy et al., 2006; Colpron et al., 2015):

1. Devonian extension and subsequent continental terrane (e.g. Yukon-Tanana, Kootenay) rifting in response to back-arc initiation driven by slab retreat (eastward dipping subduction) (Fig. 11c).
2. Late Devonian-Earliest Carboniferous post-rift subsidence with ocean sea-floor spreading (Mid-Ocean Ridge basalt) recorded in the Slide Mountain terrane (Fig. 11d).
3. Convergence recorded by a subsidence deficit during the Pennsylvanian to Early Permian that may be related to a switch off of the initial eastward dipping subsidence during the Late Carboniferous-Early Permian (Fig. 11e).
4. 1st foreland (collisional pro-foreland). Flexure and uplift recording the progressive shortening and slicing of the Slide Mountain ocean below the Yukon-Tanana and Quesnellia terranes (Late Permian) and potential isostatic

rebound induced by slab break of the west-dipping subduction (at least in the Yukon Territory) (Fig. 11f).

5. 2nd foreland (retro-foreland associated with short-lived Cache Creek subduction). Renewed eastward-dipping subduction during deposition of the Montney Fm. (Early Triassic) that could correspond to the Cache Creek subduction below the Ancestral North America margin (Fig. 11g).
6. Termination of dynamic subsidence during the Middle to Late Triassic, recording the Cache Creek entrapment, slab break off and sinking, followed by isostatic rebound and exhumation (Fig. 11h)
7. 3rd foreland (retro-foreland associated with long-lived subduction). Rejuvenating eastward-dipping subduction during the latest Triassic – earliest Jurassic and initiation of the wedge-top and foredeep depozones (e.g. Whitehorse Trough) (Fig. 11i).
8. Multi-pulsed retro-foreland evolution (Jurassic-Cretaceous), recorded by the stacking of the island arcs in the Cordillera (Fig. 11j).
9. Isostatic rebound during the Late Cenozoic.

This model of WCSB evolution has additional implications regarding large scale geodyamic evolution of the western margin of North American ancestral craton. It challenges the large geodynamic model proposed by Sigloch and Mihalynuk (2013) in two ways. First, the process to form a large slab wall could be related to mixing slabs from different origins that were detached during several subduction reversals (Slide Mountain ocean and Cache Creek). This is an alternative proposal to forming massive slab walls to an invoked stationary trench and an associated slab buckling model (Sigloch and Mihalynuk, 2013). Second, the relative timing between the arc-continent collision (Intermontane - ancestral North American margin) and the induced foreland basin should be revisited. The very first arc-

continent collision (Yukon-Tanana - Quesnellia) recorded by the Montney retro-foreland basin (Early Triassic) was not responsible for the large slab break off. It is the second main arc-continent collision during Late Triassic (Stikina) that accounts for the large slab wall.

FEEDBACK ON FORELAND INITIATION

Traditionally the initiation of a foreland basin is defined using a combination of the sediment provenance (Poulton, 1989; Leckie and Smith, 1992), the distribution of depositional environments (Beaumont, 1981), the development of a narrow basin fill parallel to the axis of the thrust belt (Jordan, 1981), and the onset of rapid subsidence (Angevine et al., 1990; Xie and Heller, 2009; McCartney, 2012). Our study using subsidence analysis of the entire basin fill shows that the WCSB and its associated Cordilleran orogen records three main foreland stages with distinctive subduction configurations: a first one during the Permian, a second one during the Early Triassic and a last one during the Jurassic to Cenozoic. The common point, regardless of the basin and plate configuration, is the very first forebulge uplift associated with the foredeep development in response to the onset of thrusting and flexural loading. While foredeep data are often inaccessible or not preserved, the best approach to identifying foreland initiation is to characterize and quantify uplift dynamics at the basin scale through backstripping to illustrate forebulge - backbulge depozones.

CONCLUSIONS

Our paper contributes to the characterization of the geodynamic setting for the Montney Formation (Early Triassic). Backstripping tectonic subsidence curves were quantified for six wells and two outcrop sections along a proximal to distal

transect that is representative of the entire Western Canada Sedimentary Basin. It proved necessary to analyze the entire sedimentary column to put the Montney Formation into a broader context and provide consistent interpretations regarding the type of subsidence and geodynamic setting for the Montney Formation.

The tectonic subsidence evolution during the deposition of the Montney Fm. is herein interpreted as a combination of the topographic loading of the orogenic wedge (flexure) and the sublithospheric ‘‘loading’’ caused by slab load-driven subsidence (dynamic subsidence). This suggests that the retro-foreland basin setting was associated with an eastward dipping subduction during the deposition of the Montney Fm..

We also show that the entire dynamic evolution of terrane interaction and the Canadian Cordillera development can be interpreted in the light of backstripped subsidence curves from multiple wells across the WCSB. Three main foreland basin stages, associated with different basin-subduction configurations, were identified. The first one (Permian) was coeval with the development of Late Paleozoic anorogenic highland referred to as the Ancestral Rockies (cf. Miall and Blakey, 2008 for review). The final foreland phase was initiated during the Late Triassic-Early Jurassic and was coeval with the breakup of Pangaea. The Early Triassic, amongst with the Montney Fm., recorded an additional foreland phase in between these two main geodynamic events.

As a perspective for future work, the backstripping subsidence data set can be interpreted to produce idealized flexural profiles, from which flexural properties of the lithosphere might be derived (DeCelles, 2012). They can also be used to estimate the velocity of migration of the flexural wave through the evolution for

the three foreland systems. Finally, the integrated interpretation could be used as a guideline to address some of the debates and challenges dealing with the Antler and Sonoma orogenies in the western United States and Ancestral Rockies.

ACKNOWLEDGEMENTS

The authors would like to acknowledge IFP Energies Nouvelles for its financial support during the "Montney Project" for the last five years. This manuscript benefited greatly from helpful constructive comments and suggestions provided by Jim Barclay, Matt Adams, Thomas Moslow.

REFERENCES

Alberta Geological Survey 2015. Alberta Table of Formations; Alberta Energy Regulator, URL <http://ags.aer.ca/document/Table-of-Formations.pdf> [September 2015].

Angevine, C.L., Heller, P.L. and Paola, C. 1990. Quantitative Sedimentary Basin Modeling: American Association of Petroleum Geologists Shortcourse Note Series #32, 247 pp.

Armitage, J.H. 1962. Triassic oil and gas occurrences in northeastern British Columbia, Canada. Journal of Alberta Society of Petroleum Geologists, v. 10, p. 35-56.

Ash, C.H. 2001. Relationship between ophiolites and gold-quartz veins in the North American Cordillera. British Columbia Geological Survey. Bulletin 108. Chap. 1. p.1-8. ISBN 0-7726-4376-8

Aukes, P.G. and Webb, T.K. 1986. Triassic Spirit River Pool, northwestern Alberta. In: Canadian Society of Petroleum Geologists, 1986 Core Conference, Calgary, Alberta, Canada. N.C. Meijer Drees (ed.). p. 3.1-3.34.

Barclay, J.E., Krause, F.F., Campbell, R.I. and Utting, J. 1990. Dynamic casting and growth faulting of the Dawson Creek Graben Complex: Carboniferous-Permian Peace River Embayment, Western Canada. In: Geology of the Peace River Arch. S.C. O'Connell and J.S. Bell (eds.). Bulletin of Canadian Petroleum Geology, v. 38A, p. 115-145.

Barresi, T., Nelson, J.L., Dostal, J. and Friedman, R.M. 2015. Evolution of the Hazelton arc near Terrace, British Columbia: Stratigraphic, geochronological, and

geochemical constraints on a Late Triassic–Early Jurassic arc and Cu-Au porphyry belt: Canadian Journal of Earth Sciences, doi:10.1139/cjes-2014-0155.

Barss, D.L., Best, E.W. and Meyers, N. 1964. Triassic, Chapter 9. In: Geological History of Western Canada. R.G. McCrossan and R.P. Glaister (eds.). Calgary, Alberta Society of Petroleum Geologists, p. 113-136.

Beaumont, C. 1981. Foreland basins: Geophysical Journal of the Royal Astronomical Society, v. 65, p. 291-329.

Beranek, L.P. and Mortensen, J.K. 2007. Investigating a Triassic overlap assemblage in Yukon: On-going field studies and preliminary detrital-zircon age data, in Emond, D.S., Lewis, L.L., and Weston, L.H., eds., Yukon Exploration and Geology 2006: Yukon Geological Survey, p. 83–92.

Beranek, L.P. and Mortensen, J.K. 2011. The timing and provenance record of the Late Permian Klondike orogeny in northwestern Canada and arc-continent collision along western North America. Tectonics, 30, TC5017.

Beranek, L.P., Mortensen, J.K., Orchard, M.J. and Ullrich, T. 2010. Provenance of North American Triassic strata from west-central and southeastern Yukon: correlations with coeval strata in the Western Canadian Sedimentary Basin and Canadian Arctic Islands. Canadian Journal of Earth Sciences, 47: 53-73.Bullard, J.E. 2009. Dust. in Geomorphology of desert environments (Parsons, A.J and Abrahams, A.D., eds) p. 629-654.

Blakey, R.C. 2014. Paleogeography and Paleotectonics of the Western Interior Seaway, Jurassic -Cretaceous of North America : AAPG Search and Discovery Article #30392. New maps, Oct. 2014. http://cpgeosystems.com/index.html

Bond, G. and Kominz, M. 1984. Construction of tectonic subsidence curves for the early Paleozoic miogeocline, southern Canadian Rocky Mountains: Implications for subsidence mechanisms, age of breakup, and crustal thinning: Bulletin of the Geological Society of America, v. 95, no. 2, p. 155.

Bonnet, S. and Crave, A. 2003. Landscape response to climate change: insights from experimental modeling and implications for tectonic vs. climatic uplift of topography. Geology 31:123–126

Campbell, C.V., Dixon, R.J. and Forbes, D.M. 1989. Updip erosional truncation of Halfway and Doig shoreline sequences: a new model for exploration in west central Alberta (Abstract). In: Exploration Update 1989 - Integration of Technologies, Programme and Abstracts. Canadian Society of Petroleum Geologists Convention, Calgary, Alberta, p. 138.

Cant, D.J. 1986. Hydrocarbon trapping in the Halfway Formation (Triassic), Wembley Field, Alberta. Bulletin of Canadian Petroleum Geology, v. 34, p. 329-338.

Catuneanu, O. 2004. Retroarc foreland systems—evolution through time. Journal of African Earth Sciences, 38, 225–242.

Chalmers, G.R.L. and Bustin, R.M. 2012. Geological evaluation of Halfway Doig Montney hybrid gas shale tight gas reservoir, northeastern British Columbia. Mar. Petrol. Geol. 38, 53e72. http://dx.doi.org/10.1016/j.marpetgeo.2012.08.004.

Clowes, R.M., Burianyk, M.J.A., Gorman, A.R. and Kanasewich, E.R. 2002. Crustal velocity structure from SAREX, the southern Alberta refraction experiment. Canadian Journal of Earth Sciences, 39: 351-373.

Cohen, K.M., Finney, S.C., Gibbard, P.L. and Fan, J-X. 2013 updated. The ICS International Chronostratigraphic Chart; Episodes 36, p. 199-204, URL <http://www.stratigraphy.org/ICSchart/ChronostratChart2015-01.pdf> [August 2015].

Colpron, M. and Nelson, J.L. 2009. A Palaeozoic Northwest Passage: Incursion of Caledonian, Baltican and Siberian terranes into eastern Panthalassa, and the early evolution of the North American Cordillera, in Earth Accretionary Systems in Space and Time, edited by P. A. Cawood and A. Kröner, Geol. Soc. Spec. Publ., 318, 273–307, doi:10.1144/SP318.10.

Colpron, M., Nelson, J.L. and Murphy, D.C. 2007. Northern Cordilleran terranes and their interactions through time: GSA Today, v. 17, p. 4-10.

Colpron, M., Crowley, J.L., Gehrels, G., Long, D.G.F., Murphy, D.C., Beranek, L. and Bickerton, L. 2015. Birth of the northern Cordilleran orogen, as recorded by detrital zircons in Jurassic synorogenic strata and regional exhumation in Yukon. Lithosphere, L451.1, first published on July 21, 2015, doi:10.1130/L451.1

Coney, P.J., Jones, D.L. and Monger, J.W.H. 1980. Cordilleran suspect terranes. Nature, v. 288, p. 329–333, doi: 10.1038/288329a0.

Crombez, V. 2016. Petrofacies, sedimentology and stratigraphic architecture of organic rich rocks. Insights from a multi- disciplinary study of the Montney and Doig Formations (Lower and Middle Triassic, Alberta – British Columbia, Canada). PhD thesis, Paris VI University, 238 p. IFPEN report 66669

Crombez, V., Rohais, S., Baudin, F. and Euzen, T., 2016. Facies, geometries and sequence stratigraphy of a wave-dominated margin: insight from the Montney Fm

(Alberta, British Columbia, Canada). Bulletin of Canadian Petroleum Geology. Volume 64, Number 4, Pages 516–537

Davies, G.R. 1997. The Triassic of the Western Canada Sedimentary Basin: tectonic and stratigraphic framework, paleogeography, paleoclimate and biota. In Triassic of the Western Canada Sedimentary Basin. Edited by T.F. Moslow and J. Wittenberg. Bulletin of Canadian Petroleum Geology, 45: 434-460.

DeCelles, P.G. and Giles, K.A. 1996. Foreland basin systems: Basin Research, v. 8, p. 105–123, doi:10.1046/j.1365-2117.1996.01491.x.

DeCelles, P. G. 2012. Foreland Basin Systems Revisited: Variations in Response to Tectonic Settings, in Tectonics of Sedimentary Basins: Recent Advances (eds C. Busby and A. Azor), John Wiley & Sons, Ltd, Chichester, UK. doi: 10.1002/9781444347166.ch20

Dickinson, W.R. 2004. Evolution of the North American Cordillera: Annual Review of Earth and Planetary Sciences, v. 32, p. 13–45, doi: 10.1146/annurev. earth.32.101802.120257.

Edwards, D.E., Barclay, J.E., Gibson, D.W., Kvill, G.E. and Halton, E. 1994. Triassic strata of the Western Canada Sedimentary Basin. In: Geological Atlas of the Western Canada Sedimentary Basin. G.D. Mossop and I. Shetsen (comps.). Calgary, Canadian Society of Petroleum Geologists and Alberta Research Council, chpt. 16

Engebretson, D. C., Cox, A. and Gordon, R. 1985. Relative motions between oceanic and continental plates in the Pacific Basin. Geol. Soc.Am. Spec. Pap. 206, 1–59.

Erdmer, P. 1987. Blueschist and eclogite in mylonitic allochthons, Ross River and Watson Lake area, southeastern Yukon. Canadian Journal of Earth Sciences, 24: 1439- 1449.

Erdmer, P., and Amstrong, R.L. 1988. Permo-Triassic dates for blueschist, Ross River area, Yukon. In Yukon geology. Vol. 2. Edited by G. Abst. Exploration and Geological Sciences, Yukon, Indian and Northern Affairs Canada, pp. 33-36.

Euzen, T., Moslow, T.F., Crombez, C. and Rohais, S. this volume. Regional Stratigraphic Architecture of the Spathian Deposits in Northeastern British Columbia – Implications for the Montney Resource Play

Faure, J.L., Osadetz, K., Benaouali, Z.N., Schneider, F. and Roure, F. 2004. Kinematic and Petroleum Modeling of the Alberta Foothills and Adjacent Foreland - West of Calgary. Oil & Gas Science and Technology – Rev. IFP, Vol. 59 (2004), No. 1, pp. 81-108

Ferri, F. 1997. Nina Creek Group and Lay Range assemblage, north-central British Columbia: Remnants of late Paleozoic oceanic and arc terranes: Canadian Journal of Earth Sciences, v. 34, p. 854–874, doi:10.1139/e17-070.

Ferri, F. and Zonneveld, J.P. 2008. Were Triassic rocks of the Western Canada Sedimentary Basin deposited in a Foreland? Canadian Society of Petroleum Geologists Reservoir, 35: 12-14

Forbes, P., Ungerer, P., Kuffus, A., Riis, F. and Enggen, S. 1991. Compositional Modeling of Petroleum Generation and Expulsion. AAPG Bulletin, 75, 873-893

Fossenier, K. 2002. Stratigraphic framework of the Pennsylvanian to Permian Belloy Formation, northeastern British Columbia: a multidisciplinary approach; M.Sc. thesis, University of Calgary, Calgary, Alberta, 292 p.

Fuentes, F., DeCelles, P. and Gehrels, G. 2009. Jurassic onset of foreland basin deposition in northwestern Montana, USA: Implications for along-strike synchroneity of Cordilleran orogenic activity: Geology, v. 37, no. 4, p. 379-382.

Gabrielse, H. 1985. Major dextral transcurrent displacements along the northern Rocky Mountain trench and related lineaments in north-central British Columbia; Geological Society of America, Bulletin, Volume 96, pages 1-14.

Gabrielse, H. and Yorath, C.J. 1989. DNAG #3. The Cordilleran Orogen in Canada. Geoscience Canada, v. 16, p. 67-83.

Gabrielse, H. 1991. Late Paleozoic and Mesozoic terrane interaction in north-central British Columbia. Canadian Journal of Earth Sciences, v. 28, p. 947-957.

Gabrielse, H., Mortensen, J.K., Parrish, R.R., Harms, T.A., Nelson, J.L. and van der Heyden, P. 1993. Late Paleozoic plutons in the Sylvester Allochthon, northern British Columbia; in Radiogenic ages and isotopic studies, Report 7, Geological Survey of Canada, Paper 93-2, pages 107-118.

Gehrels, G.E., Rusmore, M., Woodsworth, G.J., Crawford, M., Andronicos, C., Hollister, L., Patchett, P.J., Ducea, M., Butler, R.F., Klepeis, K., Davidson, C., Friedman, R.M., Haggart, J., Mahoney, J.J., Crawford, W., Pearson, D. and Girardi, J. 2009. U-Th-Pg geochronology of the Coast Mountains batholith in north-coastal British Columbia: Constraints on age and tectonic evolution: Geological Society of America Bulletin, v. 121, p. 1341–1361, doi:10.1130/B26404.1.

Gibson, D.W. and Barclay, J.E. 1989. Middle Absaroka Sequence: The Triassic Stable Craton. In: The Western Canada Sedimentary Basin - A Case History, B.D. Ricketts (ed.). Canadian Society of Petroleum Geologists, Special Publication No. 30, Calgary, Alberta, p. 219-232.

Gibson, D.W. and Edwards, D.E. 1990a. Triassic stratigraphy and sedimentary environments of the Williston Lake area and adjacent subsurface Plains, northeastern British Columbia. Field Trip Guidebook No. 6, Canadian Society of Petroleum Geologists, Basin Perspectives Conference, May 27-30, 1990, Calgary, Alberta.

Gibson, D.W. and Edwards, D.E. 1990b. An overview of Triassic stratigraphy and depositional environments in the Rocky Mountain Foothills and western Interior Plains, Peace River Arch area, northeastern British Columbia. In: Geology of the Peace River Arch. S.C. O'Connell and J.S. Bell (eds.). Bulletin of Canadian Petroleum Geology, v. 38A, p. 146-158.

Gillespie, J.M. and Heller, P.L. 1995. Beginning of foreland subsidence in the Columbian-Sevier belts, southern Canada and northwest Montana:: Geology, v. 23, no. 8, p. 723-726.

Glass, D.J. 1990. Lexicon of Canadian Stratigraphy, Volume 4, Western Canada, including Eastern British Columbia, Alberta, Saskatchewan and Southern Manitoba. Canadian Society of Petroleum Geolo- gists, Calgary, Alberta, 772 p. (note: contains numerous descriptions of all Triassic units).

Golding, M.L., Orchard, M.J. and Zonneveld, J.P. 2014a. A summary of new conodont biostratigraphy and correlation of the Anisian (Middle Triassic) strata in British Columbia, Canada. Albertiana, 42: 33-40.

Golding, M.L., Orchard, M.J., Zonneveld, J.P., Henderson, C.M. and Dunn, L. 2014b. An exceptional record of the sedimentological and biostratigraphy of the Montney and Doig formations in British Columbia. Bulletin of Canadian Petroleum Geology, 62: 157-176.

Golding, M.L., Orchard, M.J., Zonneveld, J.P. and Wilson, N.S.F. 2015. Determining the age and depositional model of the Doig Phosphate Zone in northeastern British Columbia using conodont biostratigraphy. Bulletin of Canadian Petroleum Geology, 63: 143-170.

Golding, M.L., Mortensen, F., Ferri, F., Zonneveld, J.P. and Orchard, M.J. 2016. Determining the provenance of Triassic sedimentary rocks in northeastern British Columbia and western Alberta using detrital zircon geochronology, with implications for regional tectonics. Canadian Journal of Earth Science, 53 (2), 140-155, 10.1139/cjes-2015-0082

Hammer, P.T.C. and Clowes, R.M. 1997. Moho reflectivity patterns – a comparison of Lithoprobe transects. Tectonophysics, 269, 179–198.

Harms, T.A. 1985. Cross-section through the Sylvester allochthon and underlying Cassiar platform, northern British Columbia; in Current Research, Part B, Geological Survey of Canada, Paper 85-1B, pages 341-346.

Harms, T.A. 1989. Geology of the northeast Needlepoint Mountain and Erickson mine areas, northern British Columbia (104P/A); in Geological Fieldwork 1988, B.C. Ministry of Energy, Mines and Petroleum Resources, Paper 1989-1, pages 339-344.

Hein, F.J. and McMechan, M.E. 1994. Proterozoic and Lower Cambrian Strata of the Western Canada Sedimentary Basin, in Mossop, G.D., and Shetsen, I., eds.,

Geological Atlas of Western Canada: Calgary, Canadian Society of Petroleum Geologists/ Alberta Research Council, p. 57-67.

Henderson, C.M., Richards, B.C. and Barclay, J.E. 1994. Permian strata of the Western Canada Sedimentary Basin. In: Geological Atlas of the Western Canada Sedimentary Basin. G.D. Mossop and I. Shetsen (comps.). Calgary, Canadian Society of Petroleum Geologists and Alberta Research Council, chpt. 15.

Henderson, C.M., Zubin-Stathopoulos, K., Dean, G., Spratt, D. and Chau, Y.P. 2010. Tectonic history, biostratigraphy and fracture analysis of upper Paleozoic and lowest Triassic strata of east-central British Columbia; in Geoscience BC Summary of Activities 2009, Geoscience BC, Report 2010- 1, p. 259–270, URL http://www.geosciencebc.com/i/pdf/SummaryofActivities2009/SoA2009_Henderson.pdf [2016].

Henderson, C.M., Zubin-Stathopoulos, K.D. and Dean, G.J. 2012. Chronostratigraphic and tectonostratigraphic summary of the Late Paleozoic and Early Triassic succession in east-central British Columbia (NTS 093I, O, P); in Geoscience BC Summary of Activities 2011, Geoscience BC, Report 2012-1, p. 115–124.

Hunt, A.D. and Ratcliffe, J.D. 1959. Triassic stratigraphy, Peace River area, Alberta and British Columbia, Canada. American Association of Petroleum Geologists, Bulletin, v. 43, p. 563-589.

Irving, E., Woodsworth, G.J., Wynne, P.J. and Morrison, A. 1985. Paleomagnetic evidence for displacement from south of the Coast Plutonic Complex, British Columbia. Canadian Journal of Earth Sciences, v. 22, p. 584-589.

Johnston, S.T. and Borel, G.D. 2007. The odyssey of the Cache Creek terrane, Canadian Cordillera: Implications for accretionary orogens, tectonic setting of Panthalassa, the Pacific superwell, and break-up of Pangea. Earth Planet. Sci. Lett. 253: 415–28

Jordan, T. 1981. Thrust loads and foreland basin evolution, Cretaceous, western United States: Bulletin of the American Association of Petroleum Geologists, v. 12, no. 12, p. 2506-2520.

Kominz, M.A. and Bond, G.C. 1991. Unusually large subsidence and sea level events during middle Paleozoic time: New evidence supporting mantle convection models for supercontinent assembly. Geology, v. 19, p. 56-60.

Leckie, D. and Smith, D. 1992. Regional setting, evolution, and depositional cycles of the Western Canada Foreland Basin: American Association of Petroleum Geologists Memoir, v. 55, p. 9–46.

Marsden, H. and Thorkelson, D.J. 1992. Geology of the Hazelton volcanic belt in British Columbia: Implications for the Early to Middle Jurassic evolution of Stikinia: Tectonics, v. 11, p. 1266–1287, doi:10.1029/92TC00276.

McCarney, T.M. 2012. A methodology for studying tectonic subsidence variations: insights from the Fernie Formation of west-central Alberta. Thesis (M.Sc.) -- University of Calgary (Canada), ISBN: 9780494882221

McClelland, W.C. and Gehrels, G.E. 1990. Geology of the Duncan Canal shear zone: Evidence for Early to Middle Jurassic deformation of the Alexander terrane, southeastern Alaska: Geological Society of America Bulletin, v. 102, p. 1378–1392, doi:10.1130/0016-7606 (1990) 102 < 1378 :GOTDCS >2.3.CO;2.

McKenzie, D. 1978. Some remarks on the development of sedimentary basins: Earth and Planetary Science Letters, v. 40, p. 25-32.

McLearn, F.H. and Kindle, E.D. 1950. Geology of northeast British Columbia. Geological Survey of Canada, Memoir 259.

Miall, A.D. and Blakey, R.C. 2008. The Phanerozoic tectonic and sedimentary evolution of North America, in Miall, A.D., ed., The Sedimentary Basins of the United States and Canada: Sedimentary Basins of the World, v. 5, K. J. Hsü, Series Editor, Elsevier Science, Amsterdam, p. 1-29.

Mihalynuk, M.G., Smith, M., Gabites, J.E., Runkle, D. and Lefebure, D. 1992. Age of emplacement and basement character of the Cache Creek terrane as constrained by new isotopic and geochemical data; Canadian Journal of Earth Sciences, Volume 29, pages 2463-2477.

Mihalynuk, M.G., Nelson, J. and Diakow, L.J. 1994. Cache Creek terrane entrapment: Oroclinal paradox within the Canadian Cordillera: Tectonics, v. 13, p. 575–595, doi: 10.1029/93TC03492.

Mihalynuk, M.G., Mountjoy, K.J., Smith, M.T., Currie, L.D., Gabites, J.E., Tipper, H.W., Orchard, M.J., Poulton, T.P. and Cordey, F. 1999. Geology and Mineral Resources of the Tagish Lake Area (NTS 104M/8, 9, 10E, 15 and 104N/12W), Northwestern British Columbia: British Columbia Ministry of Energy and Mines Bulletin 105, 217 p.

Monger, J.W.H. and Ross, C.A. 1971. Distribution of fusulinaceans in the western Canadian Cordillera: Canadian Journal of Earth Sciences, v. 8, p. 259–278, doi:10.1139/e71-026.

Monger, J.W.H. and Price, R.A. 1979. Geodynamic evolution of the Canadian Cordillera- progress and problems. Canadian Journal of Earth Sciences, v. 16, p. 770-791.

Monger, J. W. H., Souther, J. G. and Gabrielse, H. 1972. Evolution of the Canadian Cordillera: a plate-tectonic model, Am. J. Sci., 272, 577-602

Monger, J.W.H., Price, R.A. and Tempelman-Kluit, D.J. 1982. Tectonic accretion and the origin of the two major metamorphic and plutonic welts in the Canadian Cordillera. Geology, v. 10, p. 70-75.

Monger, J.W.H., Wheeler, J.O., Tipper, H.W., Gabrielse, H., Harms, T., Struik, L.C., Campbell, R.B., Dodds, C.J., Gehrels, G.E. and O'Brien, J. 1991. Part B. Cordilleran terranes, Upper Devonian to Middle Jurassic assemblages (Chapter 8), in Gabrielse, H., and Yorath, C.J., eds., Geology of the Cordilleran Orogen in Canada: Geological Survey of Canada, Geology of Canada 4, p. 281–327 (also Geological Society of America, The Geology of North America, v. G-2).

Monger, J.W.H. and Price, R.A. 2002. The Canadian Cordillera: geology and tectonic evolution. Canadian Society of Exploration Geophysicists Recorder, February, 17-36.

Mossop, G.D. and Shetsen, I. 1994. Geological Atlas of the Western Canada Sedimentary Basin. Canadian Society of Petroleum Geologists and Alberta Research Council. ISBN 0-920230-53-9. 510 p.

Mortensen, J.K., Beranek, L.P. and Murphy, D.C. 2007. Permo-Triassic orogeny in the northern Cordillera?: Sonoma north: Geological Society of America, Abstracts with Programs, 103rd Annual Meeting, Bellingham, Washington.

Murphy, D.C., van der Heyden, P., Parrish, R.P., Klepacki, D.W., McMillan, W., Struik, L.C. and Gabities, J. 1995. New geochronological constraints on Jurassic deformation of the western edge of North America, southeastern Canadian Cordillera; in Jurassic magmatism and tectonics of the North American Cordillera, Miller, D.M. and Busby, C. Editors, Geological Society of America, Special Paper 229, pages 159-171.

Murphy, D.C., Mortensen, J.K., Piercey, S.J., Orchard, M.J. and Gehrels, G.E. 2006. Mid-Paleozoic to early Mesozoic tectonostratigraphic evolution of Yukon-Tanana and Slide Mountainterranes and affiliated overlap assemblages, Finlayson Lake massive sulphide district, southeastern Yukon. In Paleozoic Evolution and Metallogeny of Pericratonic Terranes at the Ancient Pacific Margin of North America, Canadian and Alaskan Cordillera. Edited by M. Colpron and J.L. Nelson. Geological Association of Canada Special Paper, 45: 75-105.

Naylor, M. and Sinclair, H. 2008. Pro- vs. retro-foreland basins: Basin Research, v. 20, no. 3, p. 285-303, doi: 10.1111/j.1365-2117.2008.00366.x.

Nelson, J.L., Colpron, M., Piercey, S.J., Dusel-Bacon, C., Murphy, D.C. and Roots, C.F. 2006. Paleozoic tectonic and metallogenic evolution of the pericratonic terranes in Yukon, northern British Columbia and eastern Alaska, in Colpron, M., and Nelson, J.L., eds., Paleozoic Evolution and Metallogeny of Pericratonic Terranes at the Ancient Pacific Margin of North America, Canadian and Alaskan Cordillera: Geological Association of Canada Special Paper 45, p. 323–360.

Nelson, J.L. and Colpron, M. 2007 Tectonics and metallogeny of the Canadian and Alaskan Cordillera, 1.8 Ga to present, in Goodfellow, W., ed., Mineral deposits of Canada: A synthesis of major deposit types, district metallogeny, the evolution of

geological provinces, and exploration methods: Geological Association of Canada, Mineral Deposit Division, Special Publication 5, p. 755-792.

Ness, SM. 2001. The Application of Basin Analysis to the Triassic Succession, Alberta Basin: An Investigation of Burial and Thermal History and Evolution of Hydrocarbons in Triassic Rocks. (403). Retrieved 2014 (http://dspace.ucalgary.ca/handle/1880/40896).

Nokleberg, W.J., Parfenov, L.M., Monger, J.W.H., Norton, I.O., Khanchuk, A.I., Stone, D.B., Scotese, C.R., Scholl, D.W. and Fujita, K. 2000. Phanerozoic tectonic evolution of the Circum-North Pacific. Professional Paper 1626.U.S. Geological Survey (122 pp.).

O'Connell, S.C. 1990. The development of the Lower Carboniferous Peace River Embayment as determined from Banff and Pekisko formation depositional patterns. Bulletin of Canadian Petroleum Geology, v. 38A, p. 93-114.

Oldow, J. S., Bally, A. W., Ave Lallemant, H. G. and Leeman, W. P. 1989. Phanerozoic evolution of the North American Cordillera; United States and Canada, in Bally, A. W. and Palmer, A. R. eds., The geology of North America: an overview, The Geology of North America, Geological Society of America, v. A, pp. 139–232.

Onoue, T., Zonneveld, J.P., Orchard, M.J., Yamashita, M., Yamashita, K., Sato, H., Kusada, S., 2015. Paleoenvironmental changes across the Carnian/Norian boundary in the Black Bear Ridge section, British Columbia, Canada, Palaeogeogr. Palaeoclimatol. Palaeoecol. (2015), http://dx.doi.org/10.1016/j.palaeo.2015.10.008

Orchard, M.J. and Zonneveld, J.P. 2009. The Lower Triassic Sulphur Mountain Formation in the Wapiti Lake area: lithostratigraphy, conodont biostratigraphy and a new biozonation of the lower Olenekian (Smithian). Canadian Journal of Earth Science, 46: 757-790.

Pana, D.I. and van der Pluijm, B.A. 2015. Orogenic pulses in the Alberta Rocky Mountains: Radiometric dating of major faults and comparison with the regional tectonostratigraphic record: GSA Bulletin, v. 127, p. 480-502.

Piercey, S.J., Murphy, D.C., Mortensen, J.K. and Creaser, R. 2004. Mid-Paleozoic initiation of the northern Cordilleran marginal back-arc basin: geologic, geochemical and neodymium isotope evidence from the oldest mafic magmatic rocks in Yukon-Tanana terrane, Finlayson Lake district, southeast Yukon, Canada: Geological Society of America Bulletin, v. 116, p. 1087-1106.

Poulton, T. 1989. Upper Absaroka to Lower Zuni: the transition to the foreland basin (B. D. Ricketts, Ed.): Western Canada Sedimentary Basin: a case history,, p. 233.

Poulton, T.P., Christopher, J.E., Hayes, B.J.R., Losert, J., Tittemore, J. and Gilchrist, R.D. 1994. Jurassic and lowermost Cretaceous strata of the Western Canada Sedimentary Basin. In: Geological Atlas of the Western Canada Sedimentary Basin. G.D. Mossop and I. Shetsen (comps.). Calgary, Canadian Society of Petroleum Geologists and Alberta Research Council, chpt. 18

Price, R.A. 1994. Cordilleran tectonics and the evolution of the Western Canada sedimentary basin, in Mossop, G.D., and Shetsen, I., eds., Geological Atlas of Western Canada: Calgary, Canadian Society of Petroleum Geologists/ Alberta Research Council, p. 13–24.

Richards, B.C., Barclay, J.E., Bryan, D., Hartling, A., Henderson, C.M. and Hinds, R.C. 1994. Carboniferous strata of the Western Canada Sedimentary Basin. In: Geological Atlas of the Western Canada Sedimentary Basin. G.D. Mossop and I. Shetsen (comps.). Calgary, Canadian Society of Petroleum Geologists and Alberta Research Council, chpt. 14.

Rohais, S., Bonnet, S. and Eschard, R. 2012. Sedimentary record of tectonic and climatic erosional perturbations in an experimental coupled catchment-fan system. Basin Research, Volume 24, Issue 2, pages 198–212, DOI: 10.1111/j.1365-2117.2011.00520.x

Rohais, S. and Moretti, I. 2017. Structural and stratigraphic architecture of the Corinth rift (Greece): an integrated onshore to offshore basin-scale synthesis. In F. Roure et al. (eds.), Lithosphere Dynamics and Sedimentary Basins of the Arabian Plate and Surrounding Areas, Frontiers in Earth Sciences, p.89-120, DOI 10.1007/978-3-319-44726-1_5

Rudkiewicz, J.L., Sherkati, S. and Letouzey J. 2007. Evolution of Maturity in Northern Fars and in the Izeh Zone (Iranian Zagros) and Link with Hydrocarbon Prospectivity. In: O. Lacombe, J. Lavé, F. Roure, J. Verges, (eds.), Thrust Belts and Foreland Basins, From Fold Kinematics to Hydrocarbon Systems. Chap. 12, Springer, 229-246.

Saleeby, J. and Busby-Spera C.J. 1992. Early Mesozoic tectonic evolution of the western U.S. Cordillera; in The Cordilleran Orogen: Conterminous U.S.: Boulder, Colorado, Burchfiel, B.C., Lipman, P.W. and Zoback, M.L. Editors, Geological Society of America, The Geology of North America, DNAG volume G-3, 724 pages.

Shephard, G.E., Mueller, R.D. and Seton, M. 2013. The tectonic evolution of the Arctic since Pangea breakup — integrating constraints from surface geology and geophysics with mantle structure. Earth Sci. Rev. 124, 148–183.

Siberling, N.J. 1973. Geologic events during Permian-Triassic time along the Pacific margin of the United States; in The Permian and Triassic systems and their Mutual Boundary, Logan A. and Hills L.V., Editors, Canadian Society of Petroleum Geology, Volume 2, pages 345-362.

Sigloch, K. and Mihalynuk, M. 2013. Intra-oceanic subduction shaped the assembly of Cordilleran North America. Nature 496, 50–56. http://dx.doi.org/10.1038/nature12019.

Sinclair, H. and Naylor, M. 2012. Foreland basin subsidence driven by topographic growth versus plate subduction: Geological Society of America Bulletin, , no. November, 124, 368-37. doi: 10.1130/B30383.1.

Snyder, W.S. and Brueckner, H.K. 1985. Tectonic evolution of the Golconda Allochthon, Nevada: problems and perspectives. In Pre-Jurassic rocks in western North American suspect terranes . Edited by C .H . Stevens. Society of Economic Paleontologists and Mineralogists, Pacific Section, pp. 103 - 123.

Speed, R.C. and Sleep, N.H. 1982. Antler orogeny and Foreland Basin: a model. Geological Society of America Bulletin, 93: 815-828.

Steckler, M. S. and Watts, A. B. 1978. Subsidence of the Atlantic-type continental margins off New York: Earth and Planetary Science Letters, v. 41, p. 1-13.

Stewart, R. 1984. Stratigraphic correlation chart, northeastern British Columbia and adjacent areas. Province of British Columbia, Ministry of Energy, Mines and Petroleum Resources, Parliament Buildings, Victoria, B.C., 1 chart.

Struik, L.C., Parrish, R.R. and Gerasimoff, M.D. 1992. Geology and age of the Naver and Ste. Marie plutons, central British Columbia; in Radiogenic Age and Isotopic Studies, Report 5, Geological Survey of Canada, Paper 91-2, pages 155-162.

Tardy, M., Lapierre, H. Bosch, D., Cadoux, A. Narros, A., Struik, L.C. and Brunet, P. 2003. Le terrane de Slide Mountain (Cordillères canadiennes): une lithosphère océanique marquée par des points chauds. Canadian Journal of Earth Sciences 40: 833-852, doi.org/10.1139/e03-010

Tipper, H. W., Woodsworth G. J. and Gabrielse H. 1981. Tectonic assemblage map of the Canadian Cordillera and adjacent parts of the United States of America, Geol. Surv. Can., Map 1505A

Tozer, E.T. 1982. Marine Triassic faunas of North America: Their significance for assessing plate and terrane movements. Geologische Rundschau, v. 71, p. 1077-1104.

Tozer, E.T. 1984. The Trias and its ammonoids: the evolution of a time scale. Geological Survey of Canada, Miscellaneous Report 35.

van der Heyden, P. 1992. A Middle Jurassic to Early Tertiary Andean-Sierran arc model for the Coast belt of British Columbia: Tectonics, v. 11, p. 82–97, doi:10.1029/91TC02183.

Ungerer, P., Burrus, J. Doligez, B. Chenet, P. Y. and Bessis, F. 1990. Basin evaluation by integrated two-dimensional modeling of heat transfer, fluid flow,

hydrocarbon generation, and migration: American Association of Petroleum Geologists Bulletin, v. 74, p. 309-335.

Watts, A. B. and Ryan, W.B.F. 1976. Flexure of the lithosphere and continental margin basins: Tectonophysics, v. 36, p. 24-44.

Wheeler, J. O. and Gabrielse, H. 1972. The Cordilleran structural province, in Variations in tectonic Styles in Canada, edited by R. A. Price, and R. J. W. Douglas, pp. 1-82, Spec. Pap. Geol. Assoc. Can., 11

Wilson, N., Zonneveld, J.P. and Orchard, M. 2012. Biostratigraphy of the Montney Formation: From the Alberta and British Columbia subsurface, to the outcrop. GeoConvention 2012: Vision, p. 1-4.

Xie, X. and Heller, P.L.L. 2009. Plate tectonics and basin subsidence history: Geological Society of America Bulletin, v. 121, no. 1-2, p. 55, doi: 10.1130/B26398.1.

Ziegler, P.A., Bertotti, G. and Cloetingh, S. 2002. Dynamic processes controlling foreland development: the role of mechanical (de)coupling of orogenic wedges and forelands. In: Bertotti, G., Schulmann, K., Cloetingh, S. (Eds.), Continental Collision and the Tectono-Sedimentary Evolution of Forelands, Europ. Geophys. Soc. Stephan Mueller Spec. Publ., vol. 1, pp. 29–9

Zonneveld, J.P., MacNaughton, R.B., Utting, J., Beatty, T.W., Pemberton, S.G. and Henderson, C.M. 2010. Sedimentology and ichnology of the Lower Triassic Montney Formation in the Pedigree-Ring/Border Kahntah River area, northwestern Alberta and northeastern British Columbia. Bulletin of Canadian Petroleum Geology, 58: 115-140.

Zonneveld, J.P., Golding, M., Moslow, T.F., Orchard, M.J., Playter, T. and Wilson, N. 2011. Depositional framework of the Lower Triassic Montney Formation, west-central Alberta and northeastern British Columbia; in recovery – 2011 CSPG CSEG CWLS Convention, p. 1–4

Zubin-Stathopoulos, K.D., Dean, G.J., Beauchamp, B., Spratt, D.A. and Henderson, C.M. 2011. Tectonic evolution and paleogeography of Pennsylvanian–Permian strata in east central British Columbia (NTS 093I, O, P): implications from stratigraphy, fracture analysis and sedimentology; Geoscience BC Summary of Activities 2010, Geoscience BC Report 2011-1, p. 209–222.

Fig.1: a. Idealized cross-section showing the main morphological elements and depozones of Passive margin, Pro-foreland and Retro-foreland basins. WT: Wedge-top, FD: Foredeep, FB: Forebulge, BB: Backbulge, BE: Basin edge. Oceanic crust is represented in black, and cratonic masses in white. b1, b2 and b3 illustrate the theoretical tectonic subsidence curves for these three basin types, respectively. c. Theoretical distribution of the tectonic subsidence across the three basin types, with uplifted versus subsiding depozones (up/down arrows respectively).

Fig. 2: a. Geological map of the Canadian segment of the Cordillera including the main belts and terranes, and the Western Canada Sedimentary Basin (WCSB, Alberta and Williston basins). The black dash line shows the subcrop area where Triassic deposits are still preserved. Numbers refer to outcrop sections and wells presented in our study (see Table 1). Principal characteristics of allochthonous and pericratonic terranes in the Canadian Cordillera are from Monger et al. (1982), Gabrielse et al. (1991), Edwards et al. (1994), Price (1994), Wright et al. (1994), Clowes et al. (2002). Terranes: ST: Stikinia, CC: Cache Creek, Q: Quesnellia, YT: Yukon-Tanana, SM: Slide Mountain, K: Kootenay, NAC: North American Craton. b. Interpreted Lithoprobe profile showing the crustal geometry of the Cordillera orogeny (modified from Monger and Price, 2002).

Fig. 3: Simplified stratigraphic scheme for the Western Canada Sedimentary Basin – WCSB and age model used for backstripping subsidence curves. The stratigraphy is compiled from the Atlas of the Western Canada Sedimentary Basin (Mossop and Shetsen, 1994) and the Alberta Table of Formations (Alberta Geological Survey, 2015). The age boundaries are assigned from more recent sources (Cohen et al., 2013 updated).

Fig. 4: Triassic stratigraphic framework in the fold-and-thrust belt of British Columbia and the subsurface of Alberta (modified from Gibson, 1974, 1975; Gibson and Barclay, 1989; Davies, 1997; Golding et al., 2015; Crombez, 2016). The three 3rd order sequences of the Montney Fm. are highlighted in color. The age boundaries are assigned from more recent sources (Cohen et al., 2013 updated).

Fig. 5: Correlation panel of the Triassic and Montney Fm. from the two outcrops section in the fold-and-thrust belt of British Columbia (West) to the six wells from the subsurface of Alberta (East).

Fig. 6: Thickness map for the three 3rd order sequences of the Montney Fm. in the subsurface of British Columbia and Alberta (modified from Crombez, 2016). The migration of the maximum thickness in depocenter illustrate the progradation of the sluggish depositional wedge profile from proximal setting to the east to distal setting to the west.

Fig. 7: Backstripped tectonic subsidence curves for the two outcrops sections (1, 2) and six wells (3-8) during Early to Middle Triassic. Curves are presented in a relative position along the cumulative tectonic subsidence axis for legibility. The thickness of the black curves illustrates the error bar induced by uncertainty on paleobathymetry estimation. The thin white dash line correspond to the average evolution. See Table 1 and Fig. 2 for well location.

Fig. 8: Spatial and temporal evolution of the tectonic subsidence rate (m/Myr) during the deposition of the Montney Fm. Mean values are represented as well as the error bar (paleo-bathymetry uncertainties) for each sequences. Uplifted versus subsiding depozones are highlighted using arrows and colors (up/down arrows respectively, as well as unfilled/filled colors). Color code refers to the three main sequences. See Fig. 1 for keys.

Fig. 9: Solid (porosity corrected) siliciclastic sediment rate (sandstone, siltstone and shale) for the two outcrops sections (1, 2) and six wells (3-8) during Early to Middle Triassic. Following Late Permian very low value (by-pass and starved basin), the Montney Fm. recorded a major pulse in sediment supply in the same order of magnitude than the Jurassic collisional foreland initiation. See Table 1 and Fig. 2 for well location.

Fig. 10: Backstripped tectonic subsidence curves for the two outcrops sections (1, 2) and six wells (3-8) from Late Devonian to Recent. Curves are presented in a relative position along the cumulative tectonic subsidence axis for legibility. The thickness of the black curves illustrates the error bar induced by uncertainty on paleobathymetry estimation. Orange lines correspond to the theoretical evolution using a post-rift thermal subsidence with the Beta value based on the model of McKenzie (1978). See Table 1 and Fig. 2 for well location.

Fig. 11: Simple evolution scheme for the WCSB and associated north American margin in Canada before, during and after the deposition of the Montney Formation. See text for detailed description. Dashed rectangle shows the location of the WCSB. The colored interval corresponds to the Triassic. Arrows indicate uplift versus subsidence (vertical), as well as extension versus compression (horizontal). Terranes: ST: Stikinia, CC: Cache Creek, Q- YT: Yukon-Tanana and Quesnellia, SM: Slide Mountain, K: Kootenay, NAC: North American Craton.

Table 1: Outcrops and wells used in the present study. The sequence thicknesses are from Crombez (2016) and the paleobathymetries are from geometrical reconstruction in Crombez (2016). See Figures 2 and 6 for location.

Figure1

Click here to download Figure
Fig1_Rohaisetal_Montney_Subsidence.tif

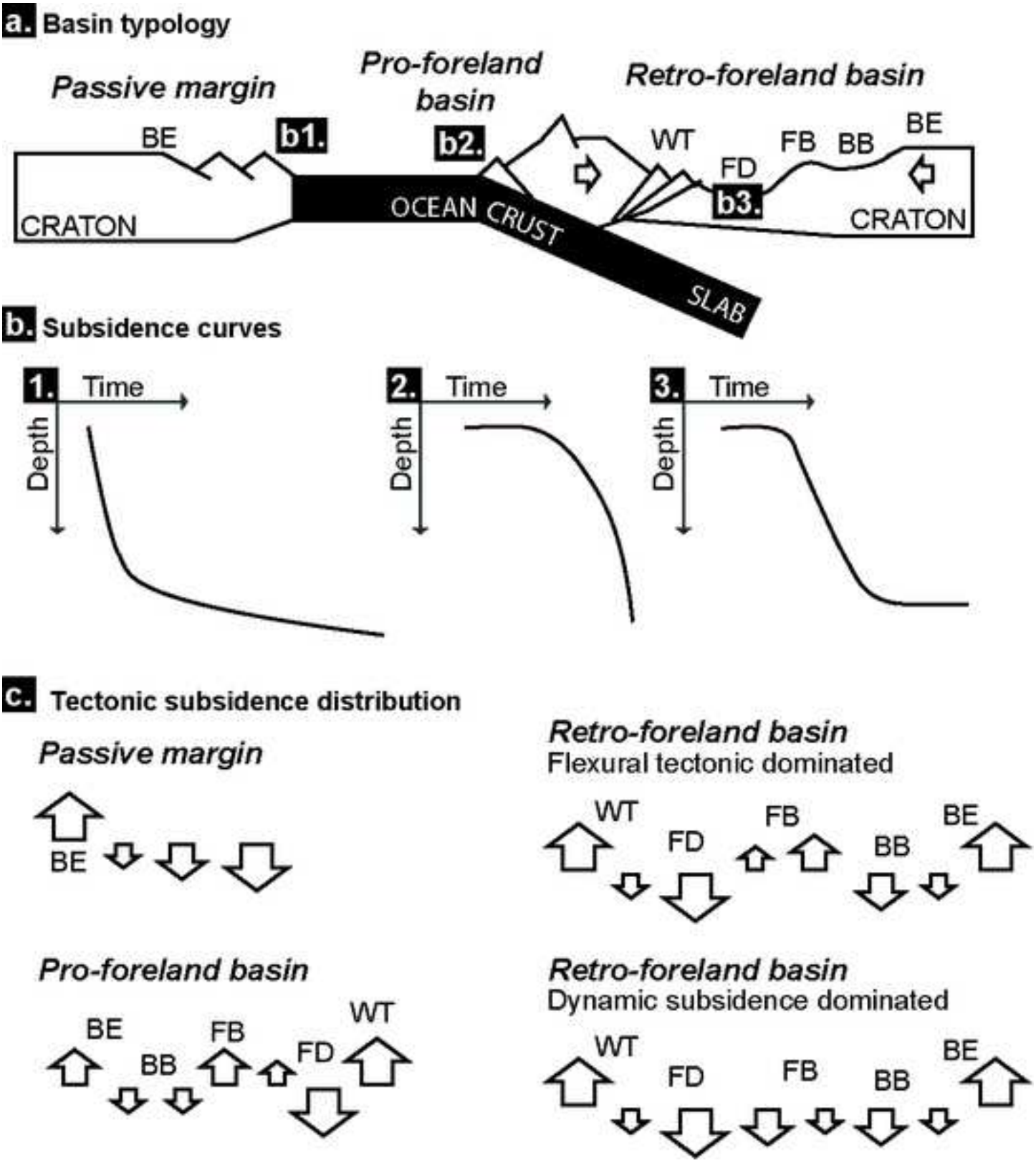

Figure2

Click here to download Figure Fig2_Rohaisetal_Montney_Subsidence.tif

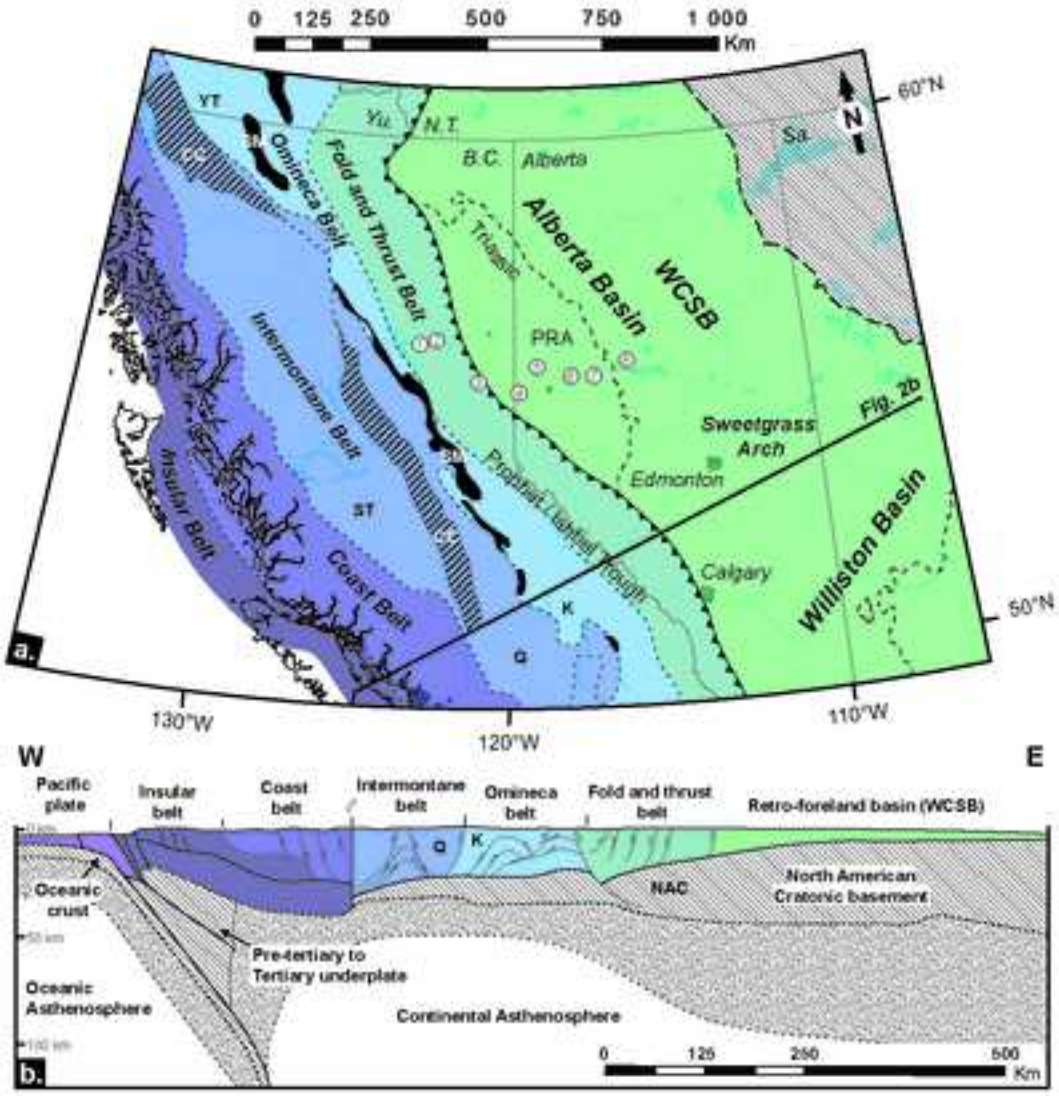

Figure3

Click here to download Figure
Fig3_Rohaisetal_Montney_Subsidence.tif

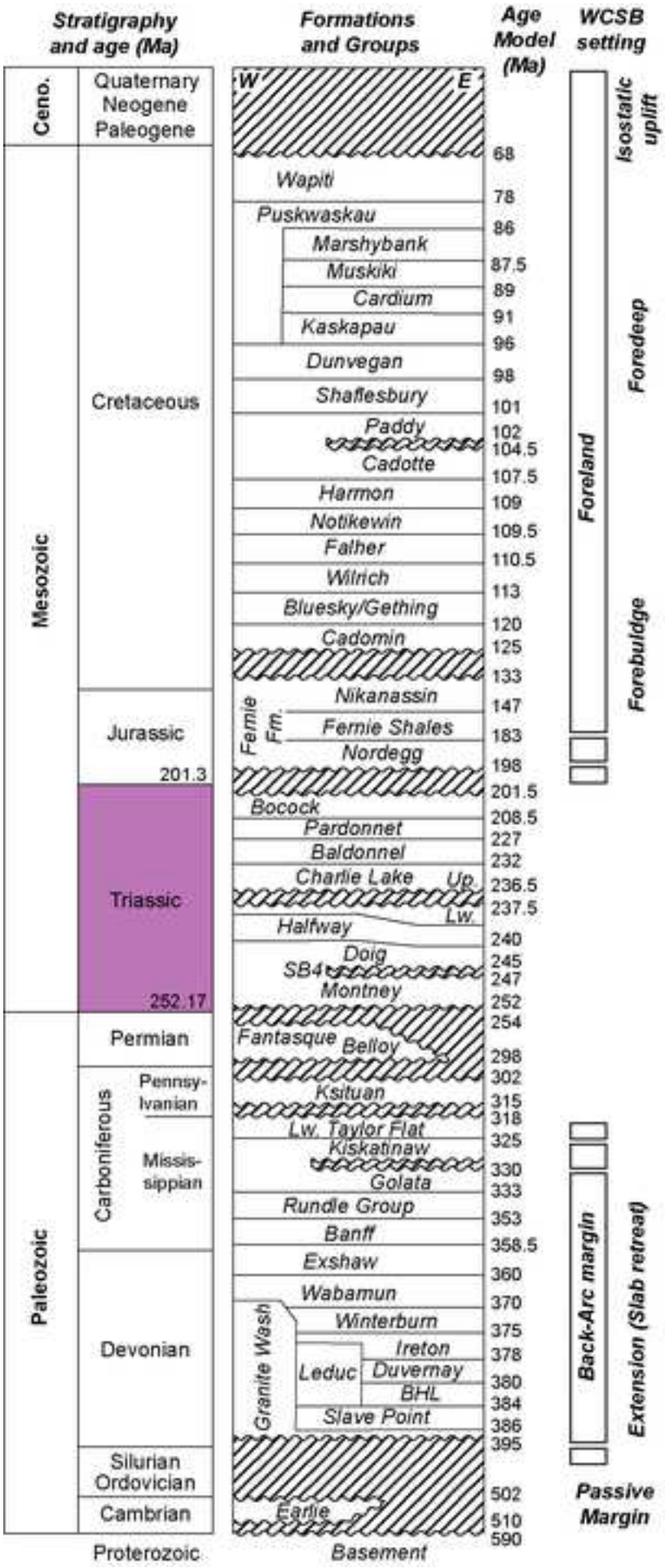

Figure4

Click here to download Figure Fig4_Rohaisetal_Montney_Subsidence.tif

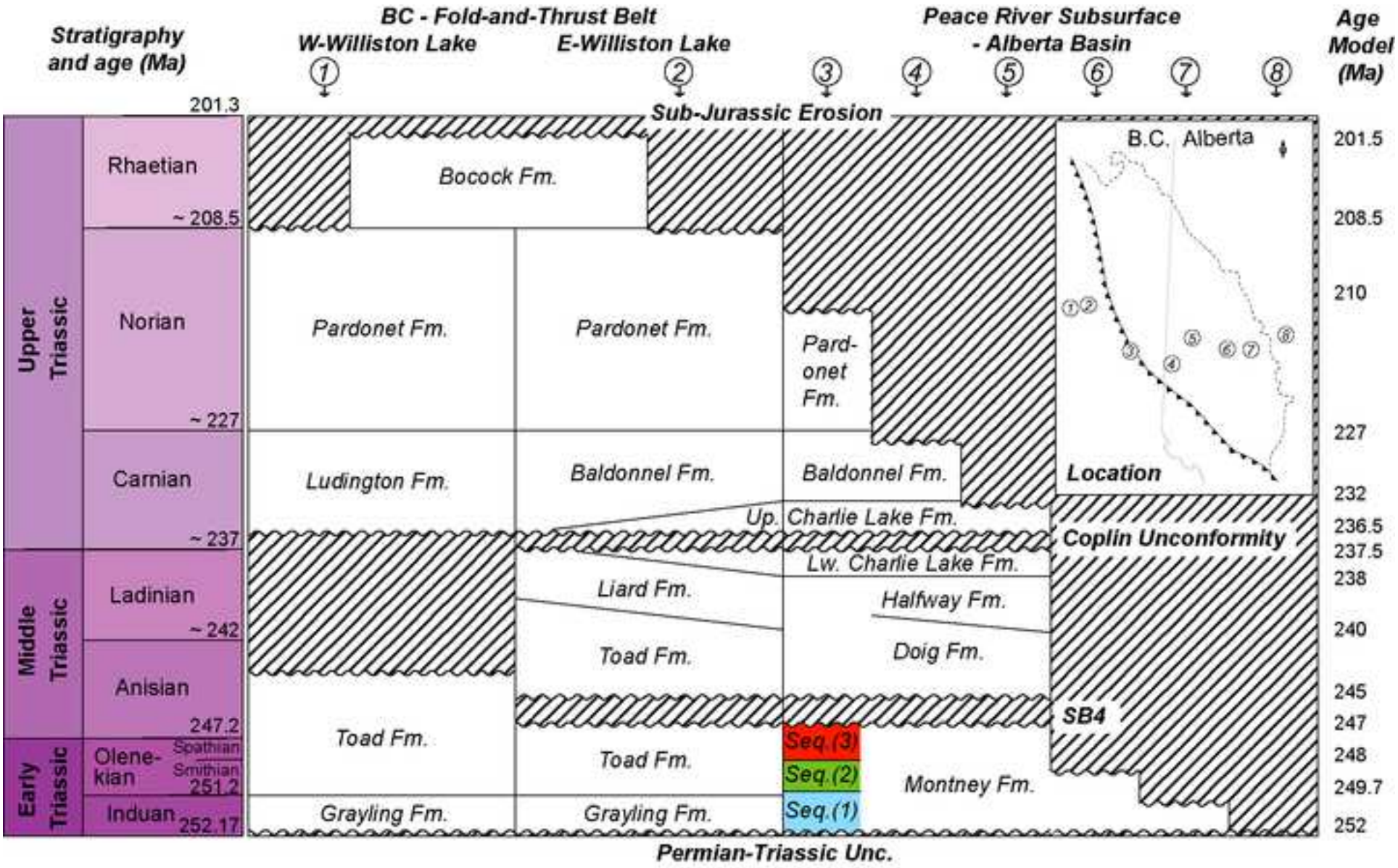

Figure5

Click here to download Figure Fig5_Rohaisetal_Montney_Subsidence.tif

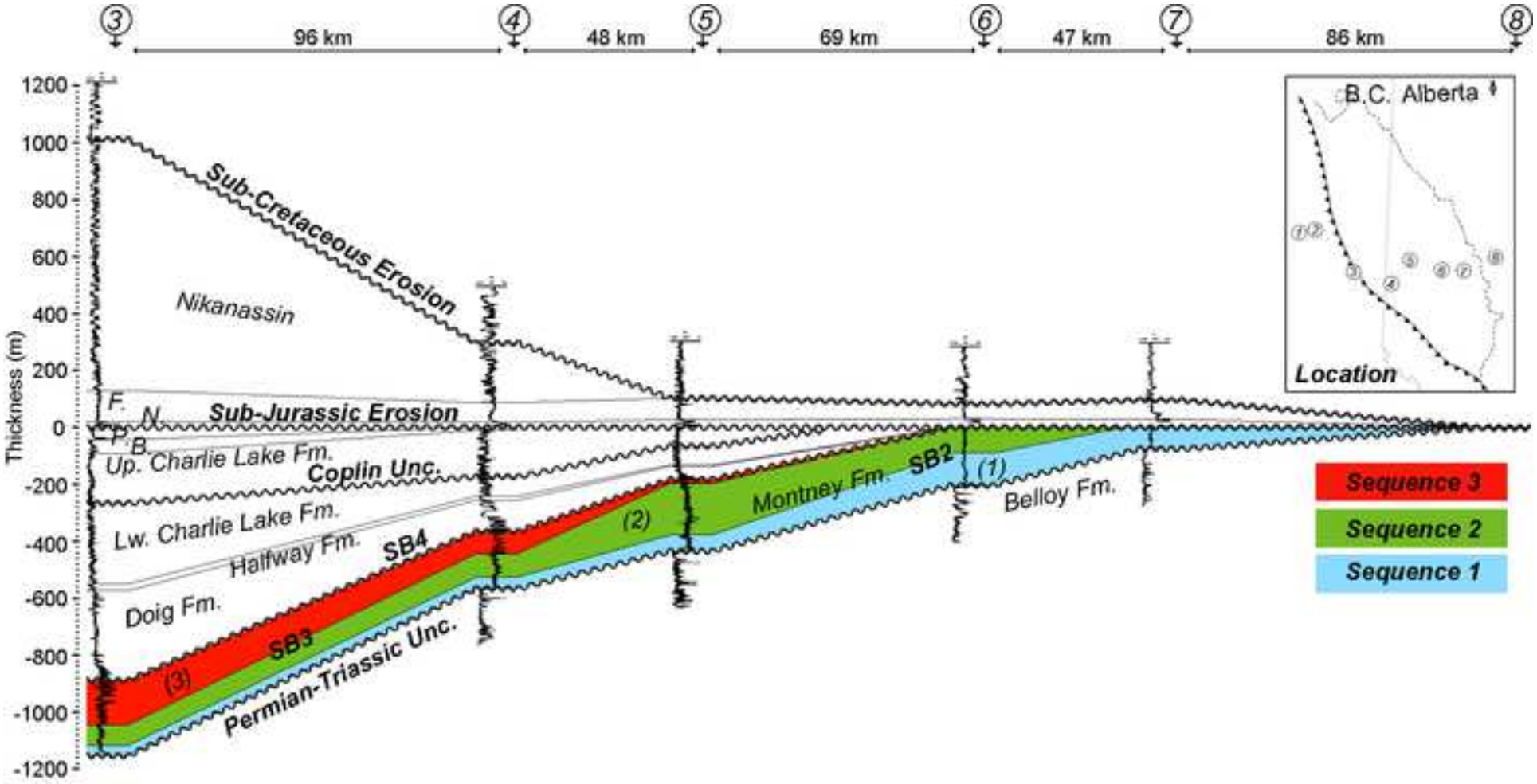

Figure6

Click here to download Figure Fig6_Rohaisetal_Montney_Subsidence.tif

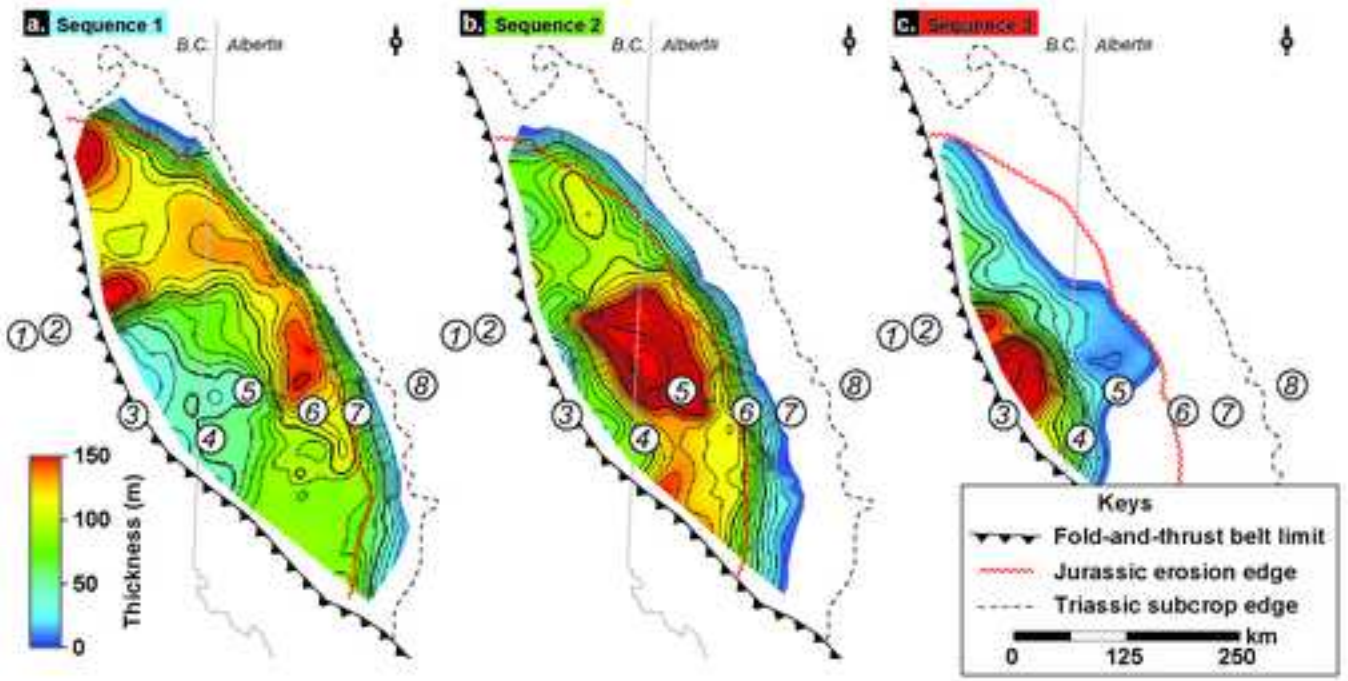

Figure7

Click here to download Figure Fig7_Rohaisetal_Montney_Subsidence.tif

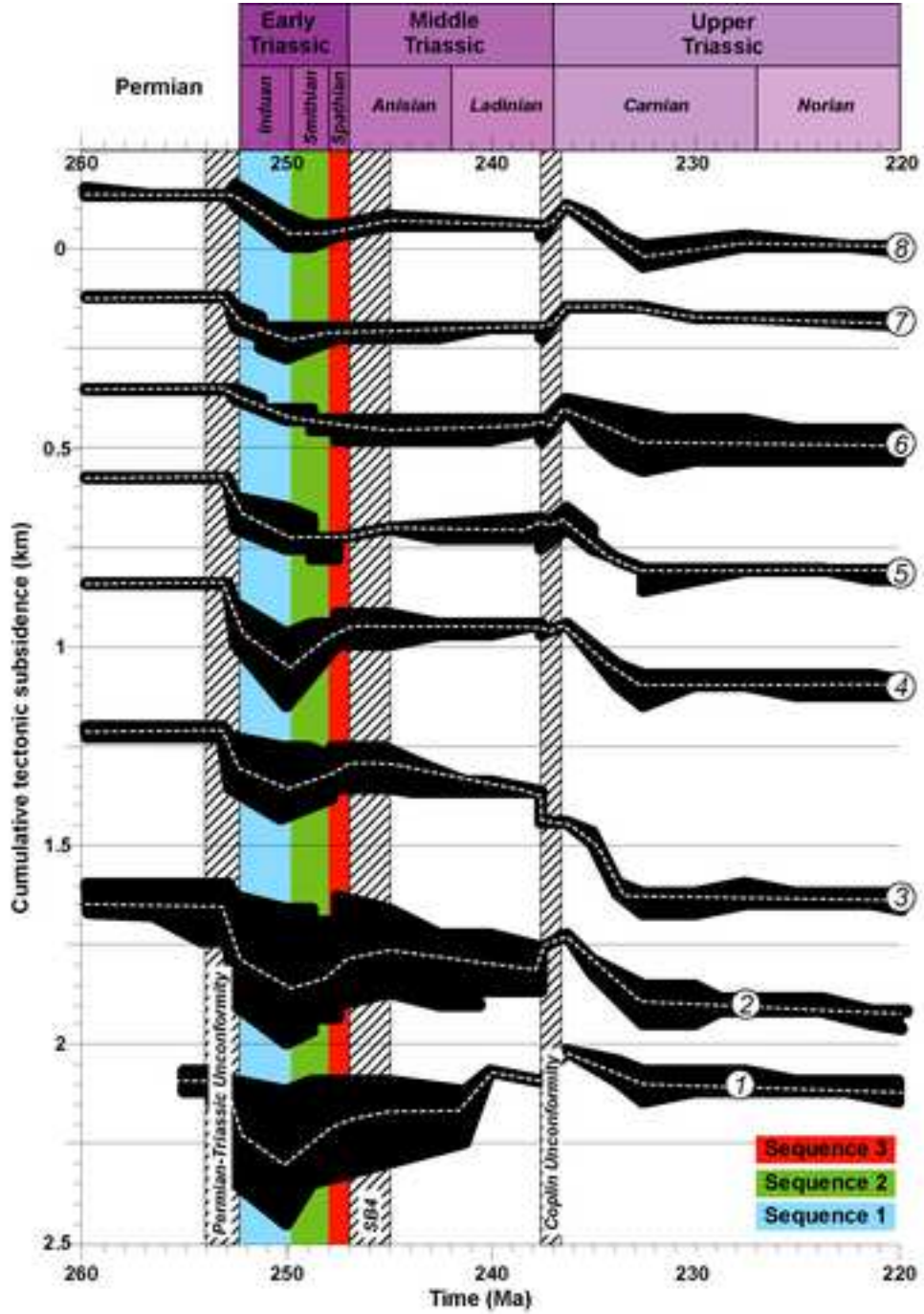

Figure8

Click here to download Figure
Fig8_Rohaisetal_Montney_Subsidence.tif

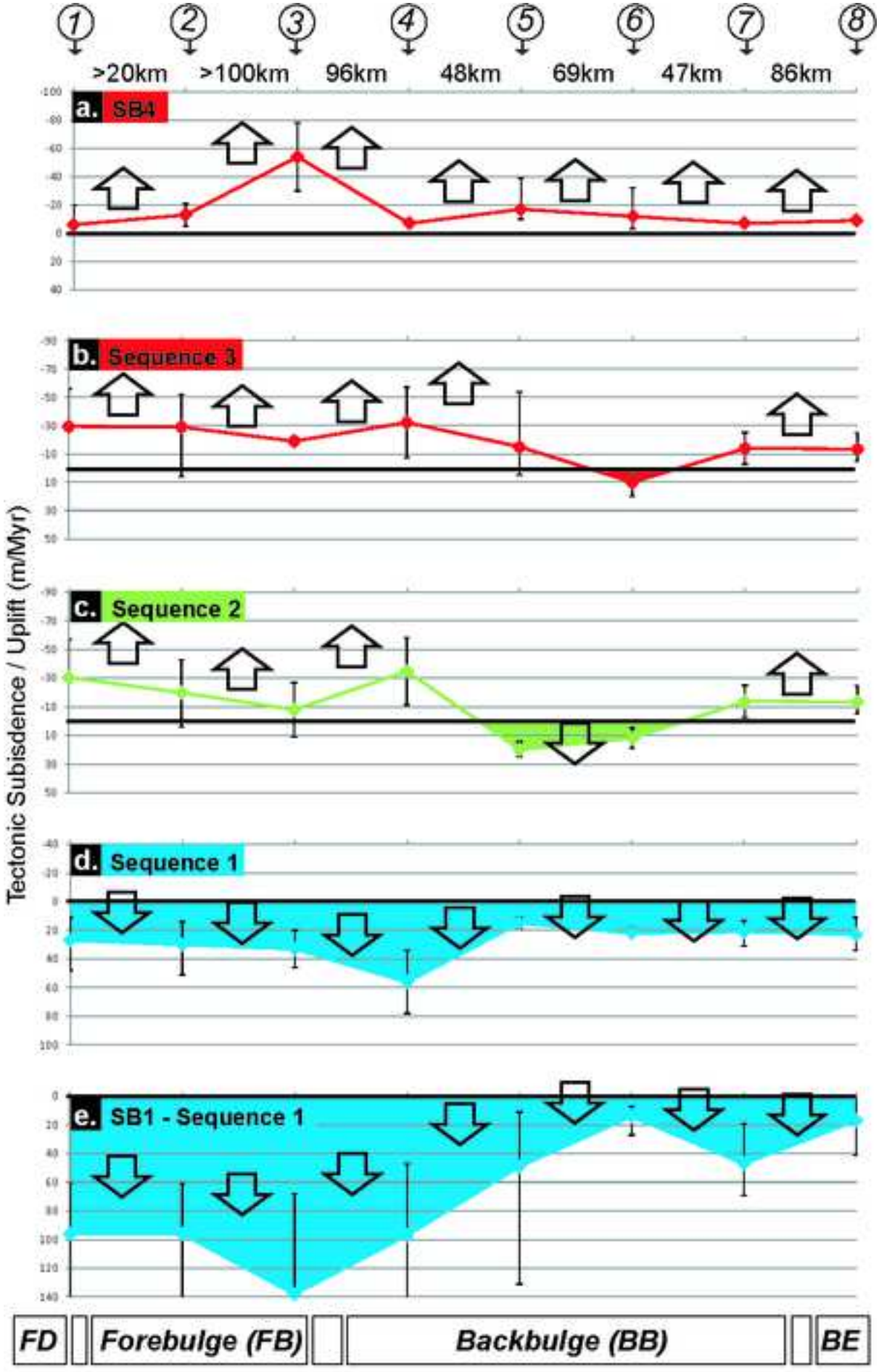

Figure9

Click here to download Figure Fig9_Rohaisetal_Montney_Subsidence.tif

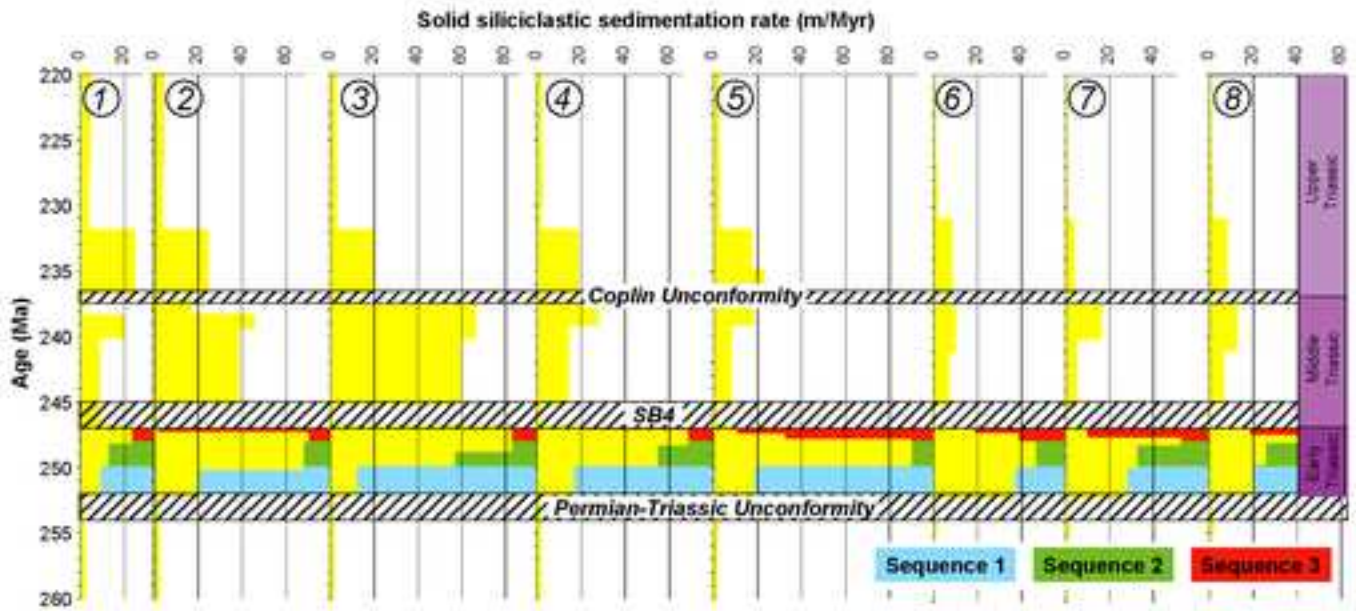

Figure10

Click here to download Figure Fig10_Rohaisetal_Montney_Subsidence.tif

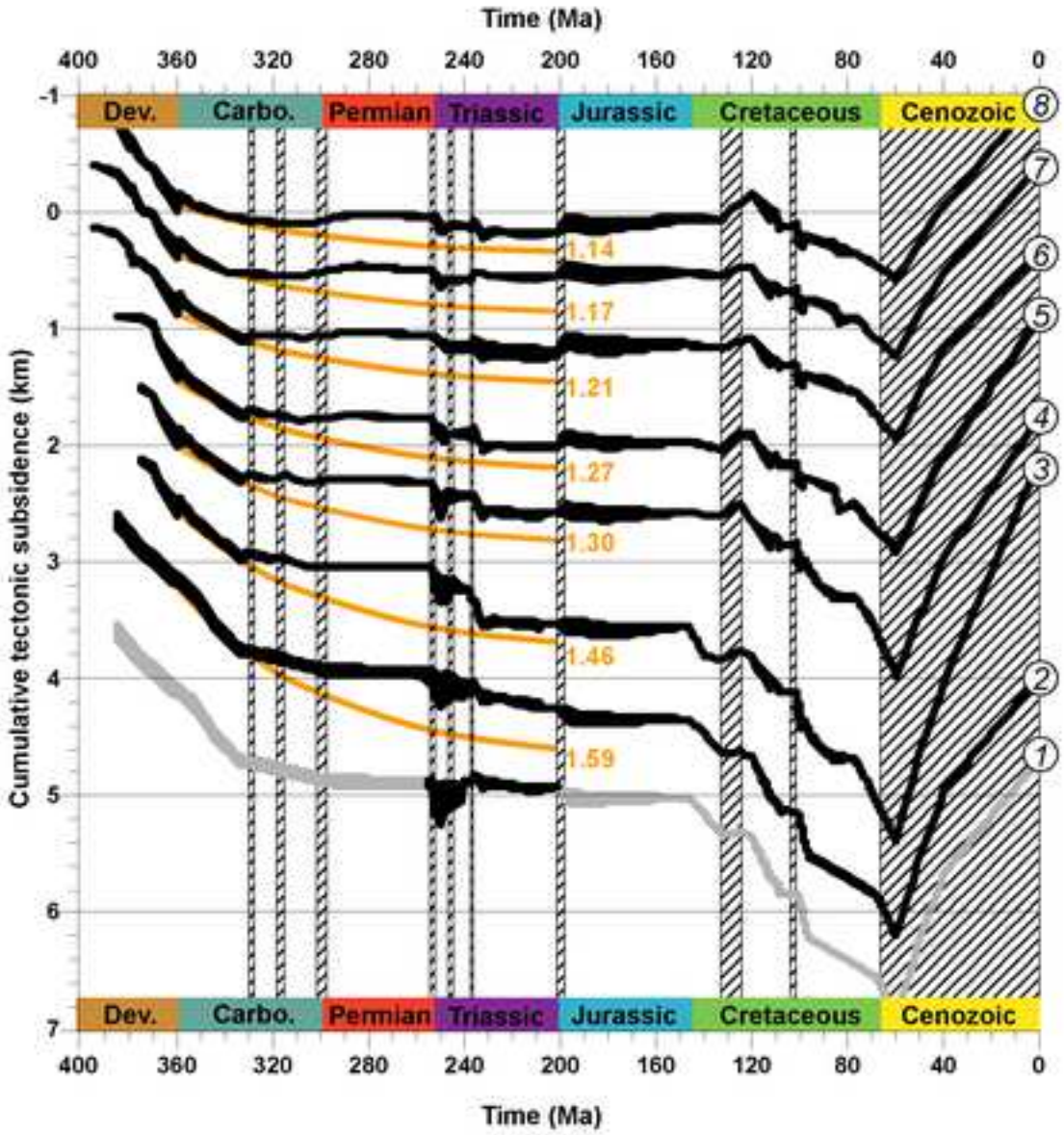

Figure11

Click here to download Figure
Fig11_Rohaisetal_Montney_Subsidence.tif

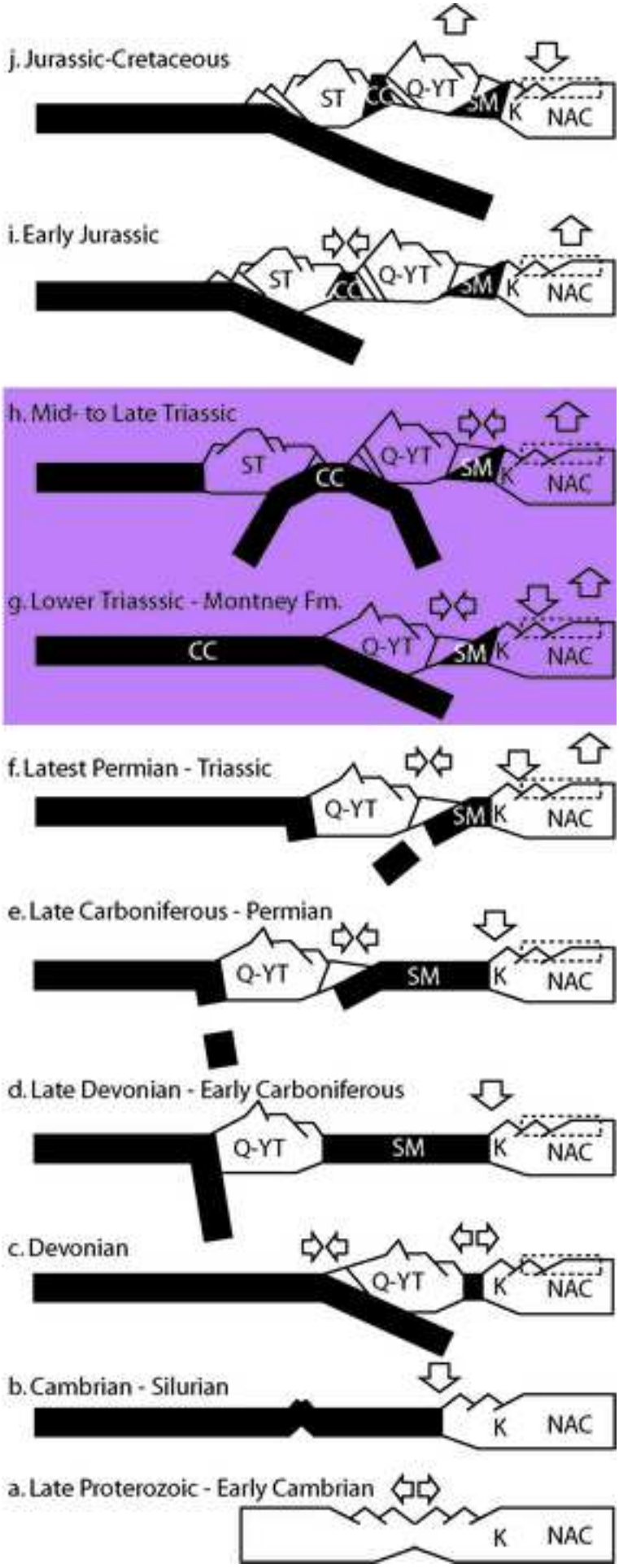

Table1

Click here to download Table Table1_Rohaisetal_Montney_Subsidence.xlsx

Number #	1	2	3	4	5	6	7	8
Name	Ursula Creek	Brown Hill	C-27-E/93-P-6	10-35-71-31W6	7-36-77-9W6	13-16-75-1W6	6-16-75-22W5	7-18-78-14W5
UWI			200C027E093P0600	100103507113W600	100073607709W600	100131607501W600	100061607522W500	100071807814W500
X (UTM)	114250	136000	597823.54	316482.82	358666.9	430501.84	477545.14	552779.15
Y (UTM)	6222650	6233460	6135411.39	6119847.71	6176286.4	6151198.12	6149686.78	6179365.95
Beta	1.66 ± 0.03	1.59 ± 0.015	1.46 ± 0.015	1.30 ± 0.01	1.27 ± 0.01	1.21 ± 0.01	1.17 ± 0.01	1.14 ± 0.01
Sequence 3								
Thickness (m)	25	2	150	63	15	25	35	40
Bathymetry (m) Average (Min-Max)	200 (50-300)	200 (50-300)	160 (80-240)	120 (60-180)	90 (45-135)	80 (40-120)	50 (25-75)	50 (25-75)
Sequence 2								
Thickness (m)	21.8	152	70	100	182	97	90	70
Bathymetry (m) Average (Min-Max)	200 (65-400)	200 (65-400)	200 (100-300)	200 (100-300)	100 (50-150)	90 (45-135)	60 (30-90)	60 (30-90)
Sequence 1								
Thickness (m)	22.5	48	30	50	57	114	85	80
Bathymetry (m) Average (Min-Max)	150 (50-300)	150 (50-300)	140 (70-210)	100 (50-150)	90 (45-135)	80 (40-120)	60 (30-90)	50 (25-75)

Appendix

Click here to download Table Appendix_Rohaisetal_Montney_Subsidence.xlsx

FORMATIONS	TYPE	PERIOD End (M.a)	Start	DEPTH Top (m)	Bottom	THICKNESS (m)
Section 1						
	U	0	0.1			
	U	0.1	40			
Erosion1	U	40	60			
Deposition1	M	60	68			
Wapiti2Kaska	M	68	96			
Dunvegan	F	96	98	0	276	276
Shaftesburry	F	98	101	276	1117	841
BoulderCreek	F	101	107.5	1117	1222	105
Hulcross	F	107.5	109	1222	1353	131
Gates	F	109	110.5	1353	1537	184
Moosebar	F	110.5	113	1537	1787	250
Gething	F	113	120	1787	2575	788
Cadomin	F	120	125	2575	2667	92
SubKErosion	U	125	128			
SubKDepositic	M	128	133			
Mont2Bick	F	133	147	2667	3784	1117
FernieShale	F	147	198	3784	4099	315
SubJurErosion	U	198	201			
SubJurDeposit	M	201	207			
BockcokDepo	F	207	208.5	4099	4160	61
PardonnetDep	F	208.5	227	4160	4293	133
Baldonnel	F	227	232	4293	4400	107
UpperCharlie	F	232	236.5	4400	4600	200
CoplinErosion	U	236.5	237.5			
LowerCharlie	M	237.5	240			
MontneyS4Er	M	240	241			
MontneyS4	F	241	245	4219	4271.5	52.5
MontneyS3	F	245	248	4271.5	4296.5	25
MontneyS2	F	248	249.7	4296.5	4318.3	21.8
MontneyS1	F	249.7	252	4318.3	4340.8	22.5
BelloyErosion	U	252	254			
BelloyDeposit	M	254	255			
Belloy	F	255	298	4340.8	4511.8	171
Stoddart	F	298	333	4511.8	5141.8	630
Debolt	F	333	353	5141.8	5850.8	709
BesaRiver	F	353	384	5850.8	6756.8	906
Section 2						
	U	0	0.1			
	U	0.1	40			
Erosion1	U	40	60			
Deposition1	M	60	68			
Wapiti2Kaska	M	68	96			

Dunvegan	F	96	98	0	276	276
Shaftesburry	F	98	101	276	1117	841
BoulderCreek	F	101	107.5	1117	1222	105
Hulcross	F	107.5	109	1222	1353	131
Gates	F	109	110.5	1353	1537	184
Moosebar	F	110.5	113	1537	1787	250
Gething	F	113	120	1787	2575	788
Cadomin	F	120	125	2575	2667	92
SubKErosion	U	125	128			0
SubKDepositic	M	128	133			0
Mont2Bick	F	133	147	2667	3784	1117
FernieShale	F	147	198	3784	4099	315
SubJurErosion	U	198	201			
SubJurDeposit	M	201	207			
BockcokDepo	F	207	208.5	4099	4160	61
PardonnetDep	F	208.5	227	4160	4293	133
Baldonnel	F	227	232	4293	4400	107
UpperCharlie	F	232	236.5	4400	4600	200
CoplinErosion	U	236.5	237.5			
LowerCharlie	M	237.5	237.75			
LowerCharlie	F	237.75	238	4600	4668	68
MontneyS4	F	238	245	4668	4923	255
SB4	U	245	247			
S3Depo	M	247	247.6			
MontneyS3	F	247.6	248	4923	4925	2
MontneyS2	F	248	249.7	4925	5077	152
MontneyS1	F	249.7	252	5077	5125	48
BelloyErosion	U	252	254			
BelloyDeposit	M	254	255			
Belloy	F	255	298	5125	5296	171
Stoddart	F	298	333	5296	5926	630
Debolt	F	333	353	5926	6635	709
BesaRiver	F	353	384	6635	7541	906

Well 3

	U	0	0.1			
	U	0.1	40			
Erosion1	U	40	60			
Deposition1	M	60	70			
Wapiti	M	70	78			
Puskwaskau	M	78	86			
Marshybank	M	86	87.5			
Muskiki	M	87.5	89			
Cardium zone	M	89	90			
Cardium	M	90	91			
Kaskapau	F	91	96	0	526	526
Dunvegan	F	96	98	526	756	230

Shaftesbury	F	98	100	756	1167	411
BFS	F	100	101	1167	1490	323
Paddy	F	101	102	1490	1576	86
MidAlbianEro	U	102	104.5			
MidAlbianDep	M	104.5	105			
Cadotte	F	105	107.5	1576	1613	37
Harmon	F	107.5	109	1613	1706	93
Notikewin	F	109	109.5	1706	1774	68
Falher	F	109.5	110.5	1774	1908	134
Wilrich	F	110.5	113	1908	2124	216
BlueSky/Gethi	F	113	120	2124	2455	331
Cadomin	F	120	125	2455	2508	53
SubKErosion	U	125	133			0
SubKDepositic	M	133	140			0
NikanassinDep	F	140	147	2508	3391	883
FernieShale	F	147	183	3391	3501	110
Nordegg	F	183	198	3501	3521	20
SubJurErosion	U	198	201.5			
SubJurDeposit	M	201.5	207			
BockcokDepo	M	207	208.5			
PardonnetDep	F	208.5	227	3521	3564	43
Baldonnel	F	227	232	3564	3628	64
UpperCharlie	F	232	236.5	3628	3790	162
CoplinErosion	U	236.5	237.5			
LowerCharlie	M	237.5	237.75			
LowerCharlie	F	237.75	238	3790	4071	281
MontneyS4	F	238	245	4071	4421	350
SB4	U	245	247			
S3Depo	M	247	247.6			
MontneyS3	F	247.6	248	4421	4571	150
MontneyS2	F	248	249.7	4571	4641	70
MontneyS1	F	249.7	252	4641	4671	30
BelloyErosion	U	252	254			
UpperBelloy	M	254	269			
KsituanErosio	U	269	302			
MUKsituanDe	M	302	306			
MidUpKsituan	F	306	312	4671	4821	150
LwKsituan	F	312	315	4821	4890	69
MissErosion	U	315	318			
MissDepositio	M	318	321			
LwTaylorFlat	F	321	325	4890	5018	128
Kiskatinaw	F	325	330	5018	5108	90
GolataErosion	U	330	331			
GolataDeposit	M	331	332			
Golata	F	332	333	5108	5118	10
Rundle	F	333	353	5118	5638	520
Banff	F	353	358.5	5638	5868	230

Exshaw	F	358.5	360	5868	5871	3
Wabamun	F	360	370	5871	6071	200
Winterburn	F	370	375	6071	6111	40
Well 4						
	U	0	0.1			
	U	0.1	40			
Erosion1	U	40	60			
Deposition1	M	60	70			
Wapiti Deposi	M	70	73			
Wapiti	F	73	78	0	430	430
Puskwaskau	F	78	86	430	616	186
Marshybank	F	86	87.5	616	637	21
Muskiki	F	87.5	89	637	663	26
Cardium zone	F	89	90	663	675	12
Cardium	F	90	91	675	707	32
Kaskapau	F	91	96	707	1212	505
Dunvegan	F	96	98	1212	1446	234
Shaftesbury	F	98	100	1446	1612	166
BFS	F	100	101	1612	1780	168
Paddy	F	101	102	1780	1810	30
MidAlbianEro	U	102	104.5			0
MidAlbianDep	M	104.5	105			0
Cadotte	F	105	107.5	1810	1834	24
Harmon	F	107.5	109	1834	1867	33
Notikewin	F	109	109.5	1867	1929	62
Falher	F	109.5	110.5	1929	2059	130
Wilrich	F	110.5	113	2059	2190	131
BlueSky/Gethi	F	113	120	2190	2347	157
Cadomin	F	120	125	2347	2567	220
SubKErosion	U	125	133			
SubKDepositic	M	133	140			
NikanassinDep	M	140	147			
FernieShale	F	147	183	2567	2636	69
Nordegg	F	183	198	2636	2654	18
SubJurErosion	U	198	201.5			
SubJurDeposit	M	201.5	207			
BockcokDepo	M	207	208.5			
PardonnetDep	M	208.5	227			
BaldonnelDep	M	227	230			
Baldonnel	F	230	232	2654	2665	11
UpperCharlie	F	232	236.5	2665	2828	163
CoplinErosion	U	236.5	237.5			
LowerCharlie	M	237.5	237.75			
LowerCharlie	F	237.75	238	2828	2896	68
MontneyS4	F	238	245	2896	3010	114
SB4	U	245	247			

S3Depo	M	247	247.6			
MontneyS3	F	247.6	248	3010	3073	63
MontneyS2	F	248	249.7	3073	3173	100
MontneyS1	F	249.7	252	3173	3223	50
BelloyErosion	U	252	254			
BelloyDeposit	M	254	256			
UpperBelloy	F	256	269	3223	3233	10
MidBelloy	F	269	294	3233	3257	24
KsituanErosio	U	294	302			
MUKsituanDe	M	302	306			
LwKsituan	F	306	315	3257	3355	98
MissErosion	U	315	318			
MissDepositio	M	318	321			
LwTaylorFl	F	321	325	3355	3380	25
Kiskatinaw	F	325	330	3380	3454	74
GolataErosion	U	330	331			
GolataDeposit	M	331	333			
Rundle	F	333	353	3454	3929	475
Banff	F	353	358.5	3929	4139	210
Exshaw	F	358.5	360	4139	4143	4
Wabamun	F	360	370	4143	4343	200
Winterburn	F	370	375	4343	4403	60

Well5						
	U	0	0.1			
	U	0.1	40			
Erosion1	U	40	60			
Deposition1	M	60	70			
WapitiDeposit	M	70	78			
PuskwaskauD	M	78	84			
Puskwaskau	F	84	86	0	591	591
Dunvegan	F	86	98	591	788	197
Shaftesbury	F	98	99.5	788	917	129
BFS	F	99.5	101	917	1066	149
Paddy	F	101	102	1066	1088	22
CadotteErosio	U	102	104.5			
CadotteDepos	M	104.5	106.5			
Cadotte	F	106.5	107.5	1088	1123	35
Harmon	F	107.5	109	1123	1147	24
Notikewin	F	109	109.5	1147	1209	62
Falher	F	109.5	110.5	1209	1382	173
Wilrich	F	110.5	113	1382	1503	121
Bluesky/Gethi	F	113	120	1503	1625	122
Cadomin	F	120	125	1625	1638	13
SubKErosion	U	125	133			
SubKdepositic	M	133	140			
Nikanassin	M	140	147			

Fernie	F	147	183	1638	1714	76
Nordegg	F	183	198	1714	1740	26
SubJurErosion	U	198	201.5			
Pardonnet	M	201.5	227			
Baldonnel	M	227	232			
UpperCharlieI	M	232	235			
UpperCharlie	F	235	236.5	1740	1805	65
CoplinErosion	U	236.5	237.5			
LowerCharlie	M	237.5	237.75			
LowerCharlie	F	237.75	238	1805	1872	67
MontneyS4	F	238	245	1872	1922	50
SB4	U	245	247			
S3Depo	M	247	247.6			
MontneyS3	F	247.6	248	1922	1937	15
MontneyS2	F	248	249.7	1937	2119	182
MontneyS1	F	249.7	252.2	2119	2176	57
BelloyErosion	U	252.2	254			
BelloyDeposit	M	254	255			
MidBelloy	F	255	269	2176	2181	5
LwBelloy	F	269	284	2181	2219	38
Kistuan	U	284	308			
MUKsituan	M	308	312			
LwKsituan	F	312	315	2219	2283	64
LwTaylorFla	F	315	325	2283	2392	109
Kiskatinaw	F	325	328	2392	2492	100
GolataErosion	U	328	330			
GolataDeposit	M	330	331			
Golata	F	331	333	2492	2511	19
Runlde	F	333	353	2511	2985	474
Banff	F	353	358.5	2985	3227	242
Exshaw	F	358.5	360	3227	3233	6
Wabamun	F	360	370	3233	3486	253
Winterburn	F	370	375	3486	3524	38
GraniteWash	F	375	385	3524	3538	14
Well 6						
	U	0	0.1			
	U	0.1	40			
Erosion1	U	40	60			
Deposition1	M	60	70			
WapitiDeposit	M	70	77			
Wapiti	F	77	78	0	10	10
Puskwaskau	F	78	86	10	433	423
Dunvegan	F	86	98	433	546	113
Shaftesbury	F	98	99.5	546	643	97
BFS	F	99.5	101	643	742	99
Paddy	F	101	102	742	749	7

CadotteErosio	U	102	104.5			
CadotteDepos	M	104.5	106.5			
Cadotte	F	106.5	107.5	749	780	31
Harmon	F	107.5	109	780	800	20
Notikewin	F	109	109.5	800	853	53
Falher	F	109.5	110.5	853	1006	153
Wilrich	F	110.5	113	1006	1131	125
Bluesky/Gethi	F	113	120	1131	1223	92
SubKErosion	U	120	133			
SubKDepositic	M	133	140			
Nikanassin	M	140	147			
Fernie	F	147	183	1223	1275	52
Nordegg	F	183	198	1275	1305	30
SubJurErosion	U	198	201.5			
Bocock	M	201.5	208.5			
Pardonnet	M	208.5	227			
Baldonnel	M	227	232			
UpperCharlie	M	232	236.5			
CoplinErosion	U	236.5	237.5			
LowCharlieDe	M	237.5	237.75			
MontneyS4	M	237.75	245			
SB4	U	245	247			
S3Deposition	M	247	247.6			
MontneyS3	M	247.6	248			
MontneyS2	M	248	248.4			
MontneyS2	F	248.4	249.7	1305	1397	92
MontneyS1	F	249.7	252.2	1397	1511	114
BelloyErosion	U	252.2	254			
BelloyDeposit	M	254	255			
MidBelloy	F	255	269	1511	1521	10
LwBelloy	F	269	284	1521	1542	21
Kistuan	U	284	308			
MUKsituan	M	308	312			
LwKsituan	F	312	315	1542	1569	27
Kiskatinaw	F	315	328	1569	1597	28
GolataErosion	U	328	330			
GolataDeposit	M	330	331			
Golata	F	331	333	1597	1620	23
Runlde	F	333	353	1620	2078	458
Banff	F	353	358.5	2078	2310	232
Exshaw	F	358.5	360	2310	2313	3
Wabamun	F	360	370	2313	2538	225
Winterburn	F	370	375	2538	2665	127
Ireton	F	375	378	2665	2679	14
Leduc	F	378	380	2679	2833	154
BHL	F	380	384	2833	2911	78
GraniteWash	F	384	395	2911	2957	46

Well 7

	U	0	0.1			
	U	0.1	40			
Erosion1	U	40	60			
Deposition1	M	60	70			
WapitiDeposit	M	70	78			
PuskwaskauD	M	78	84			
Puskwaskau	F	84	86	0	326	326
Dunvegan	F	86	98	326	451	125
Shaftesbury	F	98	99.5	451	532	81
BFS	F	99.5	101	532	613	81
Paddy	F	101	102	613	620	7
CadotteErosio	U	102	104.5			
CadotteDepos	M	104.5	107			
Cadotte	F	107	107.5	620	634	14
Harmon	F	107.5	109	634	665	31
Notikewin	F	109	109.5	665	710	45
Falher	F	109.5	110.5	710	861	151
Wilrich	F	110.5	113	861	971	110
Bluesky/Gethi	F	113	120	971	1100	129
Cadomin	F	120	125	1100	1106	6
SubKErosion	U	125	133			
SubKdepositic	M	133	140			
Nikanassin	M	140	147			
Fernie	F	147	183	1106	1174	68
Nordegg	F	183	198	1174	1202	28
SubJurErosion	U	198	201.5			
Bocock	M	201.5	208.5			
Pardonnet	M	208.5	227			
Baldonnel	M	227	232			
UpperCharlie	M	232	236.5			
CoplinErosion	U	236.5	237.5			
LowerCharlie	M	237.5	238			
MontneyS4	M	238	245			
SB4	U	245	247			
S3Deposition	M	247	247.6			
MontneyS3	M	247.6	248			
MontneyS2	M	248	249.7			
MontneyS1	F	249.7	252.2	1202	1287	85
BelloyErosion	U	252.2	254			
BelloyDeposit	M	254	255			
MidBelloy	F	255	269	1287	1306	19
LwBelloy	F	269	284	1306	1338	32
Kistuan	U	284	308			
MUKsituan	M	308	312			
Rundle2LKsitu	M	312	338			

Runlde	F	338	353	1338	1743	405
Banff	F	353	358.5	1743	1984	241
Exshaw	F	358.5	360	1984	1988	4
Wabamun	F	360	370	1988	2234	246
Winterburn	F	370	375	2234	2348	114
Ireton	F	375	378	2348	2590	242
Duvernay	F	378	380	2590	2608	18
BHL	F	380	384	2608	2670	62
SlavePoint	F	384	386	2670	2684	14
GraniteWash	F	386	395	2684	2719	35

Well 8

	U	0	0.1			
	U	0.1	40			
Erosion1	U	40	60			
Deposition1	M	60	70			
WapitiDeposit	M	70	78			
PuskwaskauD	M	78	84			
Puskwaskau	F	84	86	0	88	88
Dunvegan	F	86	98	88	243	155
Shaftesbury	F	98	99.5	243	323	80
BFS	F	99.5	101	323	403	80
Paddy	F	101	102	403	419	16
CadotteErosio	U	102	104.5			
CadotteDepos	M	104.5	107.5			
Harmon	F	107.5	109	419	444	25
Notikewin	F	109	109.5	444	476	32
Falher	F	109.5	110.5	476	623	147
Wilrich	F	110.5	113	623	702	79
Bluesky/Gethi	F	113	120	702	770	68
SubKErosion	U	120	133			
SubKdepositic	M	133	140			
Nikanassin	M	140	147			
Fernie	M	147	183			
Nordegg	M	183	198			
SubJurErosion	U	198	201.5			
Bocock	M	201.5	208.5			
Pardonnet	M	208.5	227			
Baldonnel	M	227	232			
UpperCharlie	M	232	236.5			
CoplinErosion	U	236.5	237.5			
LowerCharlie	M	237.5	238			
MontneyS4	M	238	245			
SB4	U	245	247			
S3Deposition	M	247	247.6			
MontneyS3	M	247.6	248			
MontneyS2	M	248	249.7			

MontneyS1	M	249.7	252.2			
BelloyErosion	U	252.2	254			
BelloyDeposit	M	254	255			
MidBelloy	M	255	269			
LwBelloy	M	269	284			
Kistuan	U	284	308			
MUKsituan	M	308	312			
Rundle2LKsitu	M	312	338			
Runlde	F	338	353	770	1028	258
Banff	F	353	358.5	1028	1281	253
Exshaw	F	358.5	360	1281	1286	5
Wabamun	F	360	370	1286	1566	280
Winterburn	F	370	375	1566	1695	129
Ireton	F	375	378	1695	1937	242
Duvernay	F	378	380	1937	1969	32
BHL	F	380	384	1969	2029	60
SlavePoint	F	384	386	2029	2061	32
GraniteWash	F	386	395	2061	2068	7

AMOUNT ERODED (m)	AMOUNT MISSING (m)	SANDSTONE %	SILTSTONE %	SHALE %	LIMESTONE %	DOLOMITE %
0						
0						
2700						
	1500	30	30	30	10	
	1200	28	30	25	2	3
		30	30	30	10	
		30	30	30	10	
		50	50			
		3	10	85		2
		30	30	30	3	3
		4	25	65		5
		30	25	35	1	4
		71	8	5		1
50						
	50	40	17	34		3
		40	17	34		3
		2	8	88	1	1
20						
	20	55	5		5	35
					100	
			35	15	20	30
				15		85
		16	30	12	3	23
100						
	85	16	30	12	3	23
	15		45	55		
			45	55		
		30	60	5		5
		30	60	5		5
		12	46	33	2	7
2						
	2	20	5			75
		20	5			75
		30	30		30	10
					90	10
			50	50		
0						
0						
2700						
	1500	30	30	30	10	
	1200	28	30	25	2	3

		30	30	30	10	
		30	30	30	10	
		50	50			
		3	10	85		2
		30	30	30	3	3
		4	25	65		5
		30	25	35	1	4
		71	8	5		1
50						
	50	40	17	34		3
		40	17	34		3
		2	8	88	1	1
50						
	50	55	5		5	35
					100	
			35	15	20	30
				15		85
		16	30	12	3	23
50						
	50	16	30	12	3	23
		16	30	12	3	23
			45	55		
50						
	50	30	60	5		5
		30	60	5		5
		30	60	5		5
		12	46	33	2	7
2						
	2	20	5			75
		20	5			75
		30	30		30	10
					90	10
			50	50		
0						
0						
3000						
	1633	30	30	30	10	
	1100	28	30	25	2	3
	180	3	10	85		2
	20	36	35	20		
	25	3	10	85		2
	10	46	25	15		3
	32	71	3	5		1
		3	10	85		2
		44	25	20		

		4	15	80		
		19	35	35	1	2
		30	30	30	10	
15						
	15	64	10	5	5	
		64	10	5	5	
		3	10	85		2
		41	15	25	2	3
		24	30	33		5
		4	25	65		5
		30	24	34	1	3
		70	3	5		2
150						
	150	40	17	34		3
		40	17	34		3
		2	8	88	1	1
		1	1	80	15	2
110						
	50	55	5		5	35
	60				100	
			35	15	20	30
				15		85
		16	30	12	3	23
10						
	10	16	30	12	3	23
		16	30	12	3	23
			45	55		
1						
	1	30	60	5		5
		30	60	5		5
		30	60	5		5
		12	46	33	2	7
4						
	2	20	5			75
5						
	5	10	2	3	10	75
		10	2	3	10	75
		10	2		35	53
2						
	2	35	10	10	10	35
		35	10	10	10	35
		40		30		30
15						
	15		5	90	5	
			5	90	5	
			1	23	60	12
		2	9	60	26	2

			2	78	20	
			1	3	84	11
			5	30	15	50
0						
0						
2100						
	1730	30	30	30	10	
	370	28	30	25	2	3
		28	30	25	2	3
		3	10	85		2
		36	35	20		
		3	10	85		2
		46	25	15		3
		71	3	5		1
		3	10	85		2
		44	25	20		
		4	15	80		
		19	35	35	1	2
		30	30	30	10	
25						
	25	64	10	5	5	
		64	10	5	5	
		3	10	85		2
		41	15	25	2	3
		24	30	33		5
		4	25	65		5
		30	24	34	1	3
		70	3	5		2
200						
	100	40	17	34		3
	100	40	17	34		3
		2	8	88	1	1
		1	1	80	15	2
200						
	50	55	5		5	35
	60				100	
	40		35	15	20	30
	50			15		85
				15		85
		16	30	12	3	23
25						
	25	16	30	12	3	23
		16	30	12	3	23
			45	55		
10						

	10	30	60	5		5
		30	60	5		5
		30	60	5		5
		12	46	33	2	7
5						
	5	20	5			75
		20	5			75
		55	5		5	35
75						
	75	10	2	3	10	75
		10	2		35	53
95						
	95	35	10	10	10	35
		35	10	10	10	35
		40		30		30
30						
	30		5	90	5	
			1	23	60	12
		2	9	60	26	2
			2	78	20	
			1	3	84	11
			5	30	15	50
0						
0						
1650						
	890	30	30	30	10	
	750	28	30	25	2	3
	10	3	10	85		2
		3	10	85		2
		44	25	20		
		4	15	80		
		19	35	35	1	2
		30	30	30	10	
15						
	15	64	10	5	5	
		64	10	5	5	
		3	10	85		2
		41	15	25	2	3
		24	30	33		5
		4	25	65		5
		30	24	34	1	3
		70	3	5		2
200						
	150	40	17	34		3
	50	40	17	34		3

		2	8	88	1	1
		1	1	80	15	2
320						
	110		35	15	20	30
	80			15		85
	130	16	30	12	3	23
		16	30	12	3	23
100						
	100	16	30	12	3	23
		16	30	12	3	23
			45	55		
10						
	10	30	60	5		5
		30	60	5		5
		30	60	5		5
		12	46	33	2	7
5						
	5	20	5			75
		20	5			75
		55	5		5	35
85						
	85	10	2	3	10	75
		10	2		35	53
		10	2		35	53
		40		30		30
20						
	20		5	90	5	
			5	90	5	
			1	23	60	12
		2	9	60	26	2
			2	78	20	
			1	3	84	11
			5	30	15	50
		50	30	20		
0						
0						
1550						
	930	30	30	30	10	
	620	28	30	25	2	3
		3	10	85		2
		3	10	85		2
		44	25	20		
		4	15	80		
		19	35	35	1	2
		30	30	30	10	

20						
	20	64	10	5	5	
		64	10	5	5	
		3	10	85		2
		41	15	25	2	3
		24	30	33		5
		4	25	65		5
		30	24	34	1	3
125						
	50	40	17	34		3
	75	40	17	34		3
		2	8	88	1	1
		1	1	80	15	2
380						
	70				100	
	40		35	15	20	30
	60			15		85
	120	16	30	12	3	23
100						
	100	16	30	12	3	23
	45		45	55		
10						
	10	30	60	5		5
	25	30	60	5		5
	5	30	60	5		5
		30	60	5		5
		12	46	33	2	7
5						
	5	20	5			75
		20	5			75
		55	5		5	35
95						
	95	10	2	3	10	75
		10	2		35	53
		40		30		30
20						
	20		5	90	5	
			5	90	5	
			1	23	60	12
		2	9	60	26	2
			2	78	20	
			1	3	84	11
			5	30	15	50
			5	70	25	
				5	10	85
				60	40	
		50	30	20		

0						
0						
1400						
	675	30	30	30	10	
	600	28	30	25	2	3
	125	3	10	85		2
		3	10	85		2
		44	25	20		
		4	15	80		
		19	35	35	1	2
		30	30	30	10	
36						
	36	64	10	5	5	
		64	10	5	5	
		3	10	85		2
		41	15	25	2	3
		24	30	33		5
		4	25	65		5
		30	24	34	1	3
		70	3	5		2
100						
	50	40	17	34		3
	50	40	17	34		3
		2	8	88	1	1
		1	1	80	15	2
270						
	2				100	
	8		35	15	20	30
	20			15		85
	55	16	30	12	3	23
110						
	120	16	30	12	3	23
	45		45	55		
10						
	10	30	60	5		5
	35	30	60	5		5
	90	30	60	5		5
		12	46	33	2	7
10						
	10	20	5			75
		20	5			75
		55	5		5	35
150						
	75	10	2	3	10	75
	75	10	2		35	53

			1	23	60	12
		2	9	60	26	2
			2	78	20	
			1	3	84	11
			5	30	15	50
			5	70	25	
				5	10	85
				60	40	
					85	15
		50	30	20		
0						
0						
1250						
	580	30	30	30	10	
	400	28	30	25	2	3
	270	3	10	85		2
		3	10	85		2
		44	25	20		
		4	15	80		
		19	35	35	1	2
		30	30	30	10	
50						
	50	64	10	5	5	
		3	10	85		2
		41	15	25	2	3
		24	30	33		5
		4	25	65		5
		30	24	34	1	3
375						
	20	40	17	34		3
	20	40	17	34		3
	30	2	8	88	1	1
	25	1	1	80	15	2
300						
	5				100	
	40		35	15	20	30
	50			15		85
	115	16	30	12	3	23
120						
	130	16	30	12	3	23
	45		45	55		
20						
	20	30	60	5		5
	40	30	60	5		5
	70	30	60	5		5

	80	12	46	33	2	7
60						
	10	20	5			75
	30	20	5			75
	20	55	5		5	35
155						
	75	10	2	3	10	75
	210	10	2		35	53
			1	23	60	12
		2	9	60	26	2
			2	78	20	
			1	3	84	11
			5	30	15	50
			5	70	25	
				5	10	85
				60	40	
					85	15
		50	30	20		

SALT %	COAL %	TUFF/CHERT %
	5	7
	4	
	1	
	3	2
	15	
	1	5
	1	5
16		
16		
	5	7

4
1
3 2
15

1 5
1 5

16

16
16

5 7

9

11
20

11

	1
3	5
	16
	16
3	11
2	6
	1
5	3
20	
1	5
1	5
	1

16

16
16

1	3
	1

1

5 7
5 7

9

11
20

11
1
3 5

16
16

3 11
2 6
1
5 3
20

1 5
1 5

1

16

16
16

1	3
	1
1	
5	7
	11
	1
3	5
	16
	16
3	11
2	6
	1
5	3
20	
1	5
1	5

1

16
16

16
16

1 3
1

1

5 7

11
1
3 5

16
16

3 11
2 6
1
5 3

1 5
1 5

1

16

16

1 3
1

1

5	7
	11
	1
3	5
	16
	16
3	11
2	6
	1
5	3
20	
1	5
1	5
	1

16

16

1 3
1

1

5 7

11
1
3 5

16

3 11
2 6
1
5 3

1 5
1 5

1

16

16

1 3

1

1